Semiannual Phase Report No. 3

LEAD TELLURIDE BONDING AND SEGMENTATION STUDY

Covering period
August 1, 1968 - January 31, 1969

Contract No. NAS 5-9149

Prepared by
Tyco Laboratories, Inc.
Bear Hill
Waltham, Massachusetts 02154

for

National Aeronautics and Space Administration
Goddard Space Flight Center
Greenbelt, Maryland 20771

Tyco Laboratories, Inc.
Bear Hill
Waltham, Massachusetts 02154

LEAD TELLURIDE BONDING AND SEGMENTATION STUDY

Semiannual Phase Report No. 3

Covering period
August 1, 1968 - January 31, 1969

Contract No. NAS 5-9149

by

H. Bates
F. Wald
S. Mermelstein

for

National Aeronautics and Space Administration
Goddard Space Flight Center
Greenbelt, Maryland 20771

SUMMARY

Information contained in the present report may be placed in three major categories:

(1) Constitutional Studies

(a) Metal-Silicon-Germanium Systems. Data on the Pd-Si-Ge system are presented. In particular, a suggestion of a phase diagram for the binary germanium-palladium system is made. Also, certain thoughts on the alloy chemistry of group VIII silicides and germanides are outlined.

(b) Lead Telluride Containing Systems. A correction on the PbTe-MnTe system shown in the last semiannual report is given.

(2) Testing of Tungsten Diffusion Bonded Lead Telluride

Isothermal tests are discussed, but no coherent interpretation of all these tests has been made. The most significant result here is that in a number of isolated cases p-type junctions are still intact after 10,000hours of testing. In fact, one junction tested increased from 75$\mu\Omega$ to only 240 $\mu\Omega$ after 10,000 hours of total testing. It will be attempted to arrive at a coherent interpretation of all life test results, isothermal and gradient, for the next report.

(3) Engineering Design Studies

(a) A design philosophy and drawings for a high temperature cesium vapor heater using alumina tubes is presented.

(b) A concept and a design philosophy for a modular segmented thermoelectric package using Ge-Si/PbTe is shown. Detailed drawings are enclosed and certain design studies are reported.

CONTENTS

		Page No.
	SUMMARY	i
I.	INTRODUCTION	1
II.	CONSTITUTIONAL STUDIES	3
	A. The Palladium-Silicon-Germanium System	3
	B. The Palladium-Germanium System	3
	C. General Studies on Group VIII Silicides and Germanides	8
	D. The MnTe-PbTe-SnTe System	15
III.	DESIGN OF SEGMENTED COUPLE MODULES	18
IV.	ISOTHERMAL LIFE TESTING	43
V.	FEASIBILITY OF USING CESIUM PLASMA LAMPS AS HIGH TEMPERATURE TEST SOURCES	50
VI.	REFERENCES	53
	APPENDIX - Thermoelectric Building Block Drawings	54

LIST OF ILLUSTRATIONS

Fig. No.		Page No.
1	Initial layout of alloys in the ternary system palladium-silicon-germanium.	4
2	Differential thermal analysis trace of alloy $(PdGe)_{.75}(PdSi)_{.25}$.	5
3	Differential thermal analysis apparatus.	6
4	Preliminary phase diagram of the palladium-germanium system.	7
5	Differential thermal analysis trace of alloy $Pd_{85}Ge_{15}$, annealed for 65 hours at 600°C.	9
6	75 at % Pd, 25 at % Ge as cast, 200X, etched in aqua regia.	10
7	80 at % Pd, 20 at % Ge as cast, 100X, etched in aqua regia.	11
8	85 at % Pd, 15 at % Ge, as cast, 200X, etched in aqua regia.	12
9	Stability fields for group VIII silicides and germanides of $VIII_2$-IV stoichiometry.	13
10	Stability fields for group VIII silicides and germanides of VIII-IV stoichiometry.	14
11	Lattice parameter vs. concentration in sodium chloride type PbTe-MnTe solid solutions at 400°C and 550°C.	17
12	Thermoelectric building block (sub-module) scale: 2/1.	20
13	Sub-module building block arrays.	22
14	Couple mounting concept (floating couples).	25
15	Assembly stages in precision sweating of shoes to segmented couples.	29
16(a)	Couple shoe sweating fixture no. 567-201.	30
16(b)	Shoe tinning fixture no. 567-202	31
16(c)	Couple shoe sweating fixture (couple in place).	32

LIST OF ILLUSTRATIONS (Cont.)

Fig. No.		Page No.
17	Inspection procedure for checking the parallelism of surfaces "A" and "B" of the couple shoe sweating fixture.	34
18	Steady state temperature differentials within module	37
19	3P-W contacts showing material bonded to W after fracture of elements.	48
20	Schematic cross-section of preliminary design for cesium plasma heater.	51

I. INTRODUCTION

The widespread use of thermoelectric power generation has been anticipated for some years as the solution to a number of specialized power supply problems. However, the application of thermoelectrics has been hindered by a number of major materials problems. These problems can be divided into those associated with (1) the physical characteristics, (2) the chemical behavior, and (3) the low conversion efficiency of thermoelectric materials.

The predominantly covalent nature of most thermoelectric alloys results in materials which are generally weak and brittle. In addition, PbTe alloys have a high thermal expansion coefficient which leads to susceptibility to thermal shock and thermal stress cracking. The mismatch in expansion coefficient between PbTe and metals also causes a fundamental physical incompatability which must be dealt with in contacting these materials at the hot side. The vapor pressure of PbTe alloys precludes operation in vacuum or requires encapsulation. Porosity in sintered PbTe not only contributes to its mechanical instability, but may also pose a substantial long-term hazard to the integrity of metallurgical bonds by migration of the pores in the temperature gradient. The high temperature mechanical properties of PbTe alloys are very poorly defined, and there is almost a complete lack of understanding as to what role they may have in generator design.

The reactive nature of one or more elements in all thermoelectric materials places severe limitations on the materials for use as hot side contacts. Reaction between the metal contact and the thermoelectric material can produce electrically active or mechanically destructive phases at the interface. Interactions between the dopants and contacts, which can drastically affect the electrical properties, are also possible. In fact, the consequences of reaction between the thermoelectric material and any of the several materials which constitute its environment are such that extreme care must be exercised in the choice of all such materials. However, without a basic knowledge of the interactions of the thermoelectric material with metals, potential brazes,

insulations, and so forth, selection of these materials can only be by a trial and error process.

The low efficiency of thermoelectric generating materials has been the main impediment to their wider application as power sources. The search for new materials has been largely abandoned. However, the need for higher efficiencies still exists. The most feasible means for achieving higher efficiencies appears to be the combination of existing materials over extended temperature ranges. The best known thermoelectric power generation materials, PbTe and Si-Ge, have optimum temperature ranges which complement each other for operation over a temperature interval of 800-1000°C to 200-50°C. Devices utilizing these materials over such a temperature interval should exhibit higher conversion efficiency than either material alone.

Withthe beginning of the new contract period, a basic change in emphasis has occurred. The design and actual construction of operational segmented modules of SiGe/PbTe has been adopted as the major objective of the contract. The modules are experimental to the extent that they are to serve as test beds for single couples at the same time that their performance as units is to be evaluated. Thus, they are to be instrumented such that thermoelectric characteristics of each couple can be measured as a function of time. As a result of this new direction, mechanical engineering design now constitutes the major effort of the contract and metallurgical questions, particularly on PbTe, are given less emphasis.

The basic metallurgical efforts to be expended in the new contract period center solely around ternary phase diagrams of pertinent metal-silicon-germanium systems. A small effort is directed towards a study of the feasibility of using cesium vapor lamps in single crystal sapphire housings as long-term high temperature heaters for thermoelectric testing.

II. CONSTITUTIONAL STUDIES

The major effort in constitutional studies has been shifted to metal-germanium-silicon systems. Because the Pt-metals, in particular palladium, have been suggested as brazes[1] and are indeed used in some Ge-Si thermoelements of German manufacture, the investigation of the Pd-Ge-Si system was undertaken. The remainder of the work performed on MnTe-PbTe is described as well.

A. The Palladium-Silicon-Germanium System

The initial layout of alloys in the system is shown in Fig. 1. However, differential thermal analysis runs on some selected alloys (Fig. 2) revealed difficulties in the interpretation in the absence of temperature data on the binary Pd-Ge system. Thus, an investigation of the latter system had to be undertaken.

B. The Palladium-Germanium System

Information on the palladium germanium system thus far known[2, 3] is generally based on the work of Schubert and co-workers [4, 5, 6] who discovered most of the compounds in the system and determined most of their crystal structures. However, information on melting points, eutectics, etc., is given only in very rough terms, and no phase diagram could be constructed from these results.

Differential thermal analysis runs were therefore performed in our new DTA apparatus (T&T Controls Co., Media, Penna., model no. 16A) shown in Fig. 3. The design of this apparatus is based on principles developed by Dr. Paul Garn[7] now first president of the newly formed North American Thermal Analysis Society.

From the results of these runs in conjunction with the literature results and metallographic investigation of as-cast specimens, the phase diagram shown in Fig. 4 was constructed. Since the DTA apparatus was until now limited to ~ 1200° maximum temperature (a 1600°C furnace has been received), the high temperature portion around the compound Pd_2Ge is somewhat uncertain. (The melting point of Pd_2Ge itself was determined with our older temperature vs. time apparatus.)

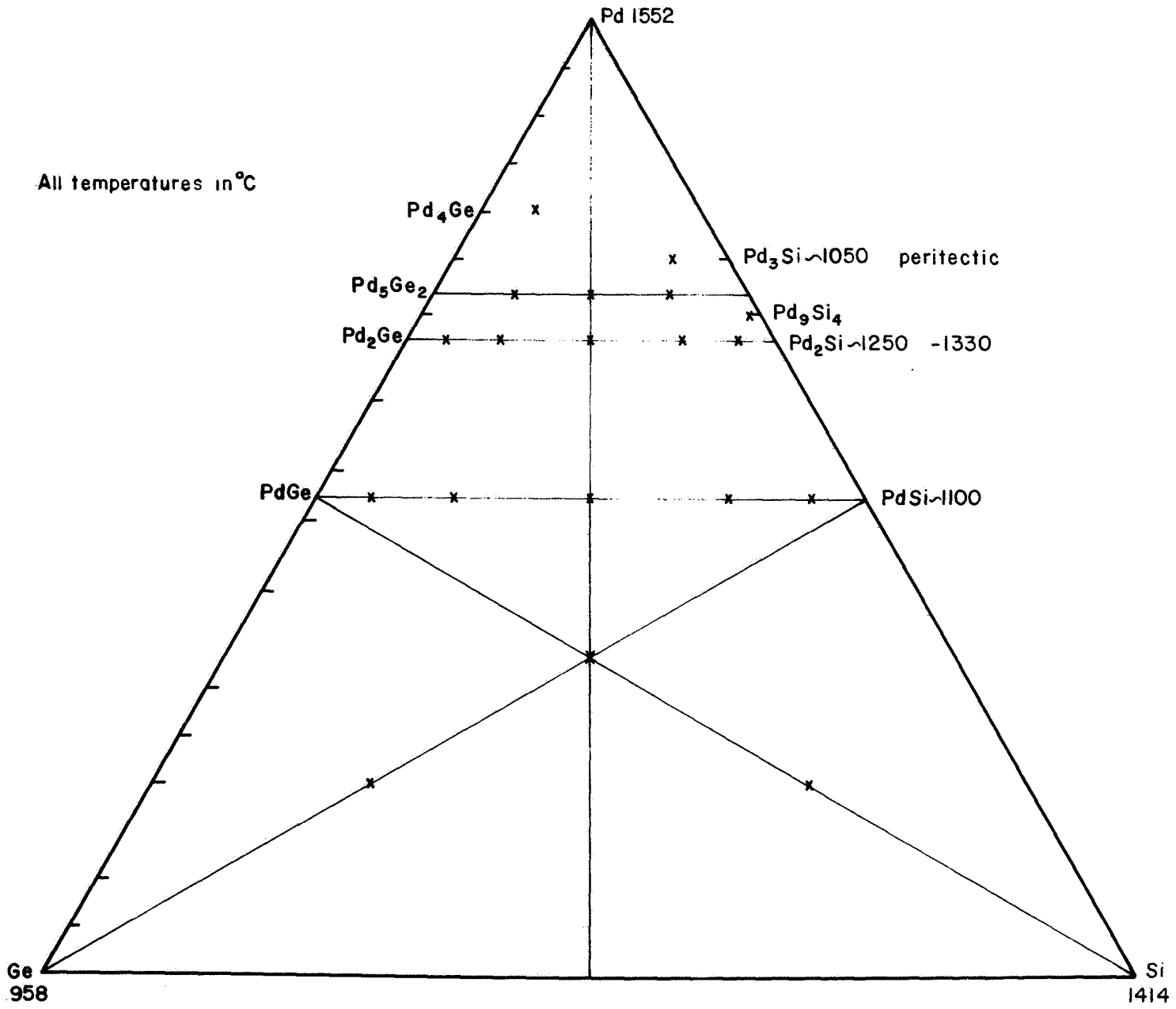

Fig. 1 Initial layout of alloys in the ternary system palladium-silicon-germanium.

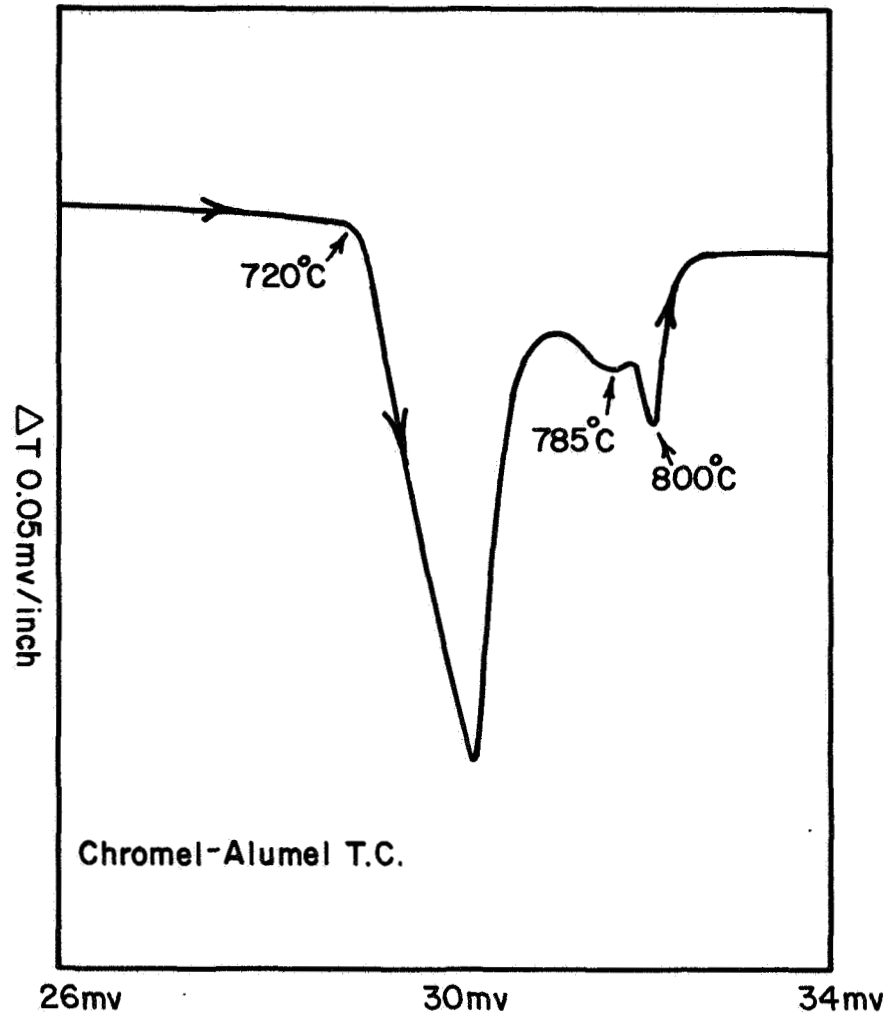

Fig. 2 Differential thermal analysis trace of alloy $(PdGe)_{.75}(PdSi)_{.25}$. Heating rate, 4°C/min; reference material, $MoSi_2$; total alloy charge, ~ 2 grams. Besides the effects shown, the alloy shows another effect at ~ 965°C. The magnitude of that effect is very strongely dependent on the heating or cooling rate and the general thermal pretreatment. Equally dependent on these factors are the sizes and shapes of the peaks shown here, indicating reactions not going to equilibrium.

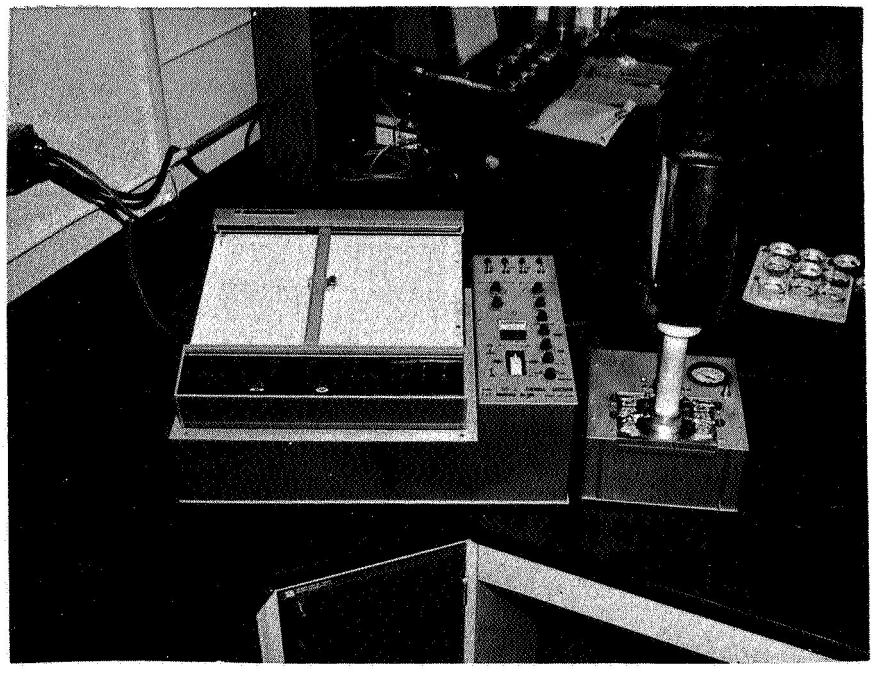

Fig. 3 Differential thermal analysis apparatus (T&T Controls Co., Media, Penna., model no. 16A).

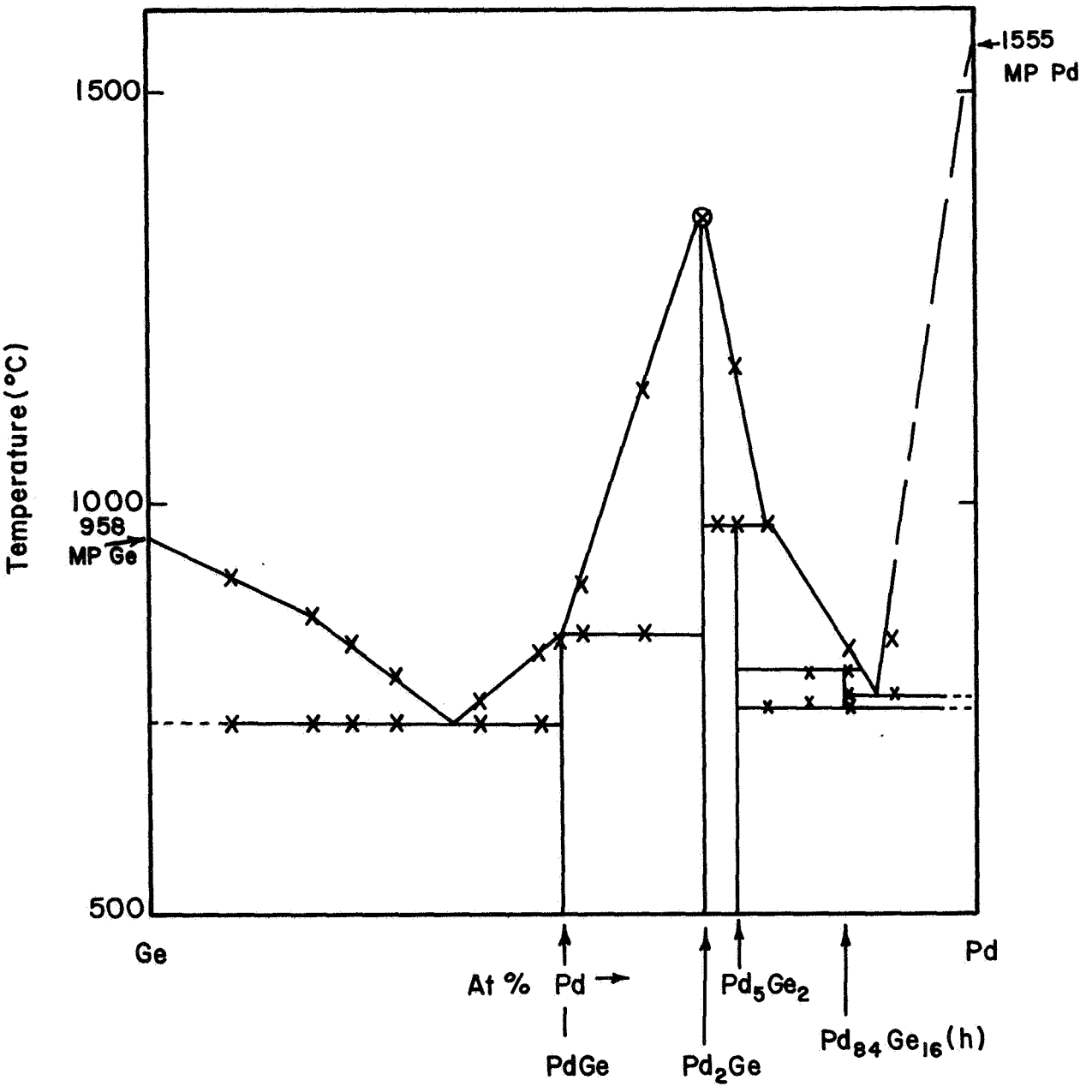

Fig. 4 Preliminary phase diagram of the palladium-germanium system.

A few remarks on this phase diagram are appropriate, although it is not considered final in the present form. The very low eutectics (725°C and 745°C respectively) not only on the Ge but also on the Pd side, are somewhat surprising. They will likely result in very low eutectics in the ternary Pd-Ge-Si system.

The compound $Pd_{84}Ge_{16}$ mentioned already by Schubert, et al.[5], can be considered as confirmed, although its exact location may still be somewhat uncertain. It is apparently formed by a peritectic reaction and decomposes eutectoidally. The DTA-thermogram of the alloy with 85 at % Ge indicates this (Fig. 5) and metallography confirms its existence there (Figs. 6, 7, 8), although no annealing has been conducted yet. The latter fact has also precluded the determination of solid solubilities of the compounds as well as the two end members. Work on the system is expected to be finalized during the next report period.

C. General Studies on Group VIII Silicides and Germanides

Some interesting behavior in the Co-Si-Ge system reported in the last phase report (this work will be pursued further, at least on a theoretical level), together with the surprising findings of the very high melting point of Pd_2Ge, prompted some general evaluation of compounds in systems of the iron and platinum metals. Such considerations may lead to useful generalizations in the present context.

Figures 9 and 10 show two plots of valence electron concentration vs. radius ratios of ($VIII_2$-IV) and (VIII-IV) compounds, respectively. The ordinates represent valence electron concentrations for the alloys in which all s and p electrons as well as the d electrons of the transition metal are counted.

The abscissae show the atomic radii ratios of the group IV elements (metallic radii for 12 coordination) to those of the transition metals. Finally, the lengths of the bars denote the melting point ratios (melting point compound/melting point transition metal). It may be stated that no correlations for the latter ratios have yet been found.

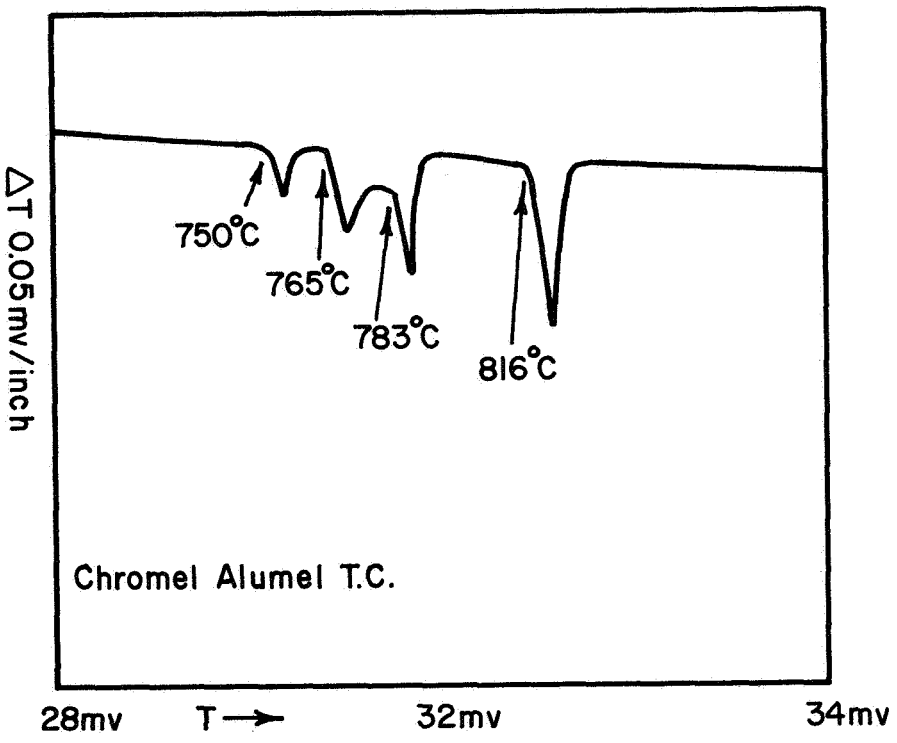

Fig. 5 Differential thermal analysis trace of alloy $Pd_{85}Ge_{15}$, annealed for 65 hours at 600° C. Heating rate, 2° C/min; reference material, alumina; total alloy charge, ~ 2 grams. Four peaks indicate that for a binary system the alloy must be located between the peritectic compound and the eutectic and also must contain a fourth transformation. The interpretation of the peaks starting at the highest temperature thus is as follows: primary crystallization, peritectic temperature, eutectic temperature, eutectoidal decomposition.

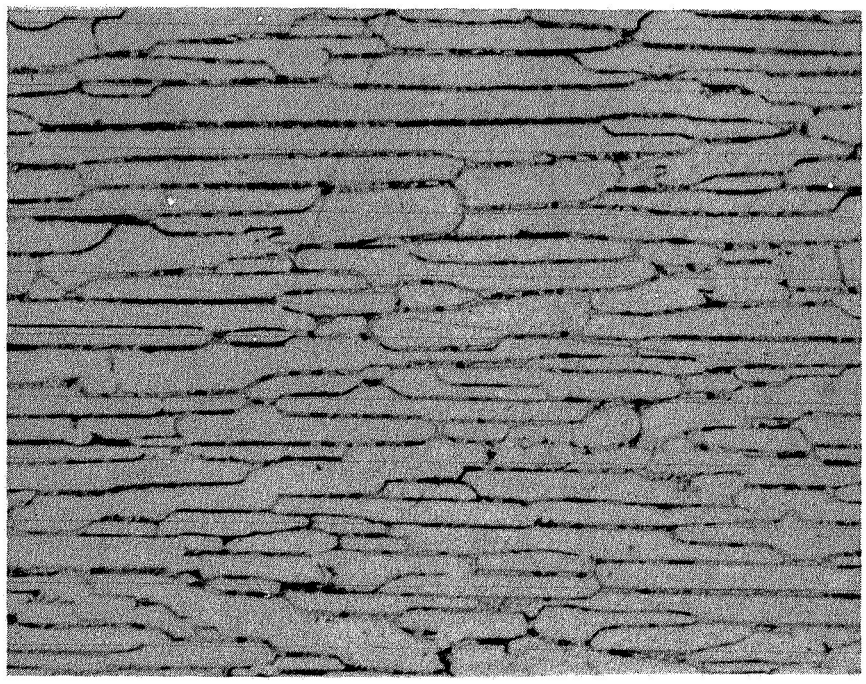

Fig. 6 75 at % Pd, 25 at % Ge as cast, 200X, etched in aqua regia. The alloy shows two-phase behavior according to the phase diagram shown in Fig. 4. The matrix should be Pd_5Ge_2 and the grain boundary phase should show eutectoidal behavior, which it does.

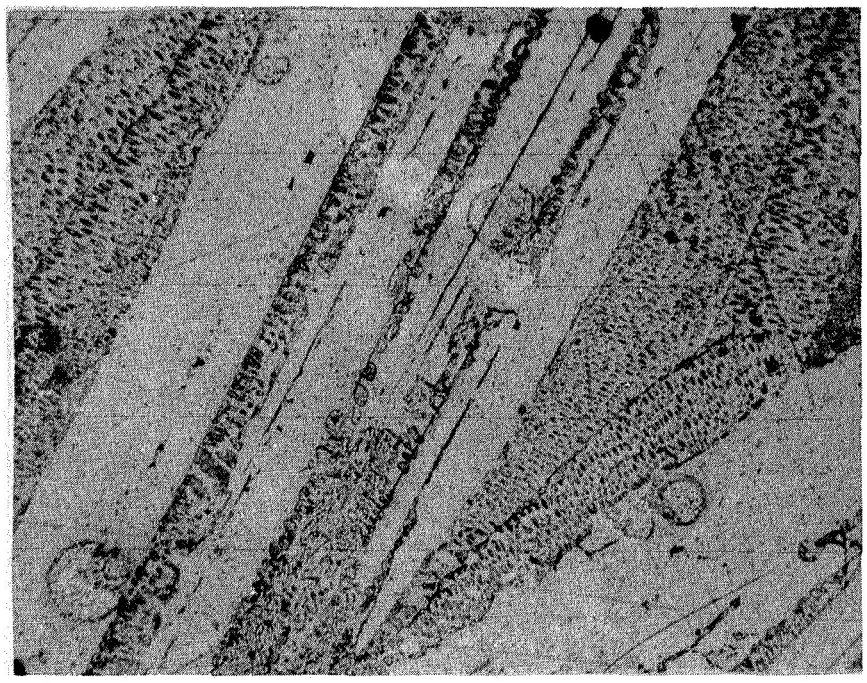

Fig. 7 80 at % Pd, 20 at % Ge as cast, 100X, etched in aqua regia. This structure, if the phase diagram construction in Fig. 4 is correct, should consist of Pd_5Ge_2 (white bars) and a eutectoidal decomposition product. Here a point of doubt arises since the structure between the bars is too coarse to be safely considered a eutectoid. Also, it is very dissimilar from the eutectoid seen in Fig. 8.

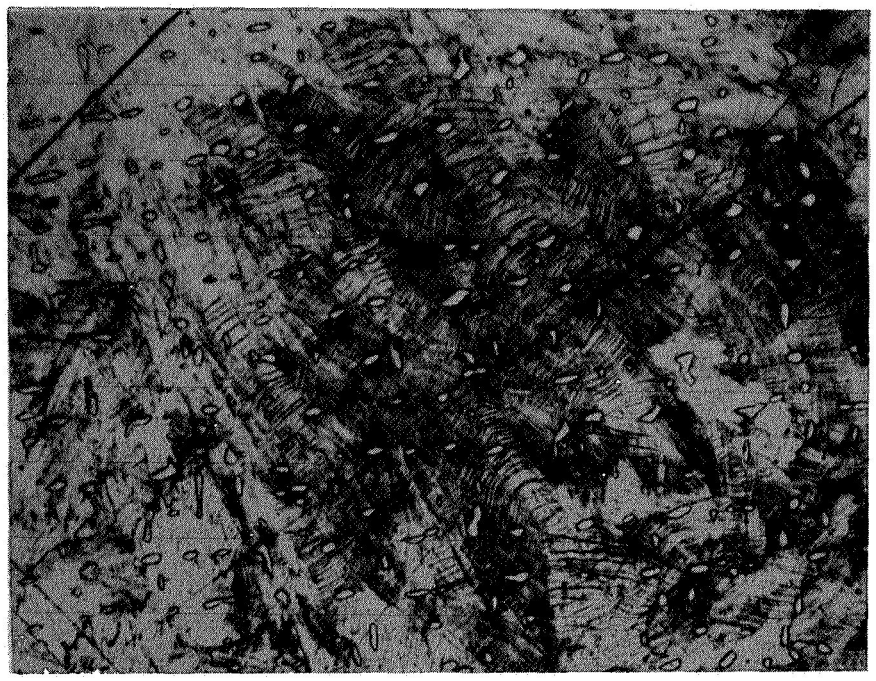

Fig. 8 85 at % Pd, 15 at % Ge, as cast, 200X, etched in aqua regia. A eutectic is seen where the matrix shows a striated transformation. This is interpreted to be the eutectoidal decomposition of $Pd_{84}Ge_{16}$. However, as expressed in Fig. 7, the area needs more detailed confirmation by annealing, controlled cooling, etc., before a final decision can be reached on its constitution.

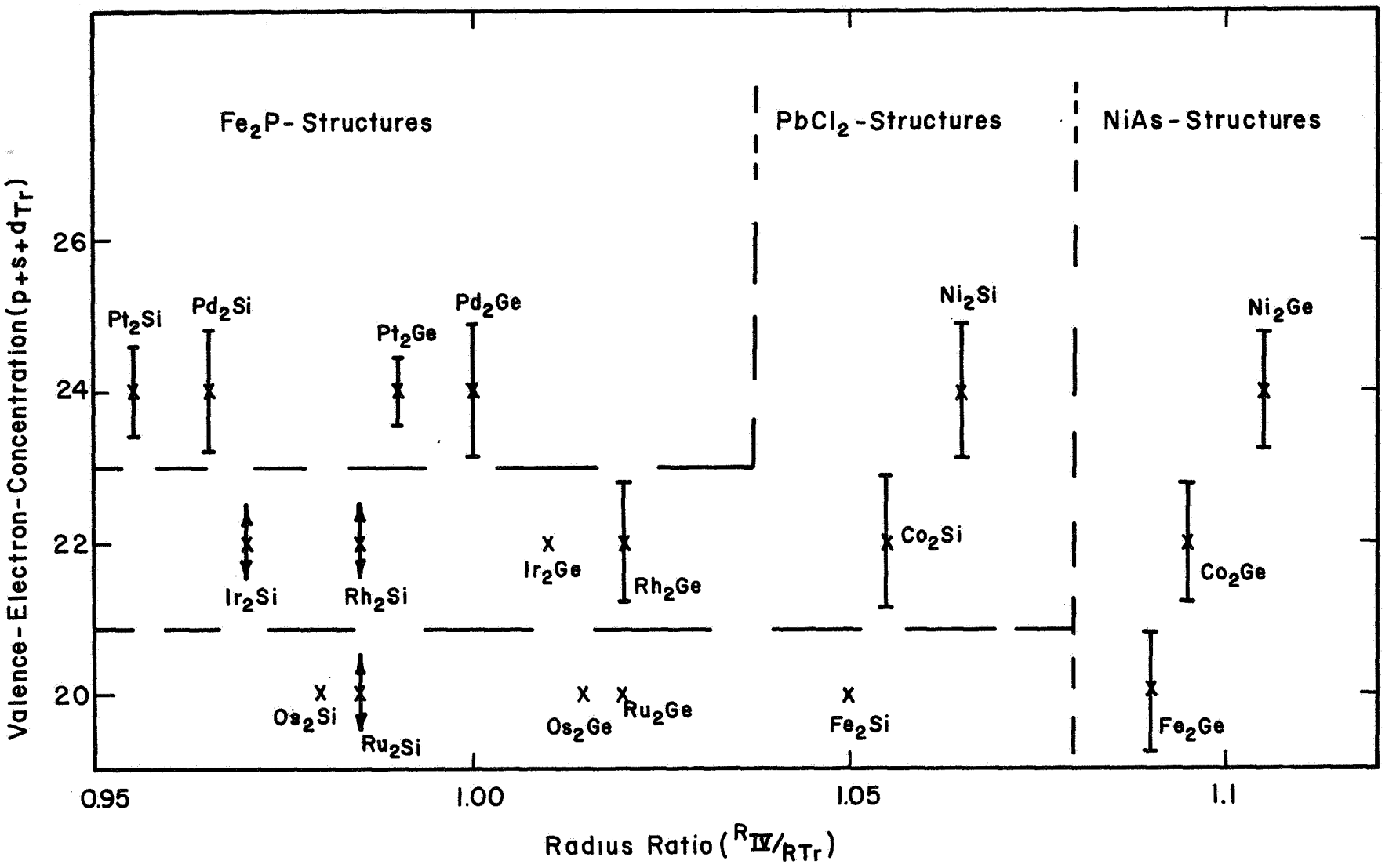

Fig. 9 Stability fields for group VIII silicides and germanides of $VIII_2$-IV stoichiometry.

x without bar = Compounds not found or extremely unstable.

= Ratio of melting point of compound to melting point of metal. Ratio of 1 = 2 cm.

= Unknown melting point ratio.

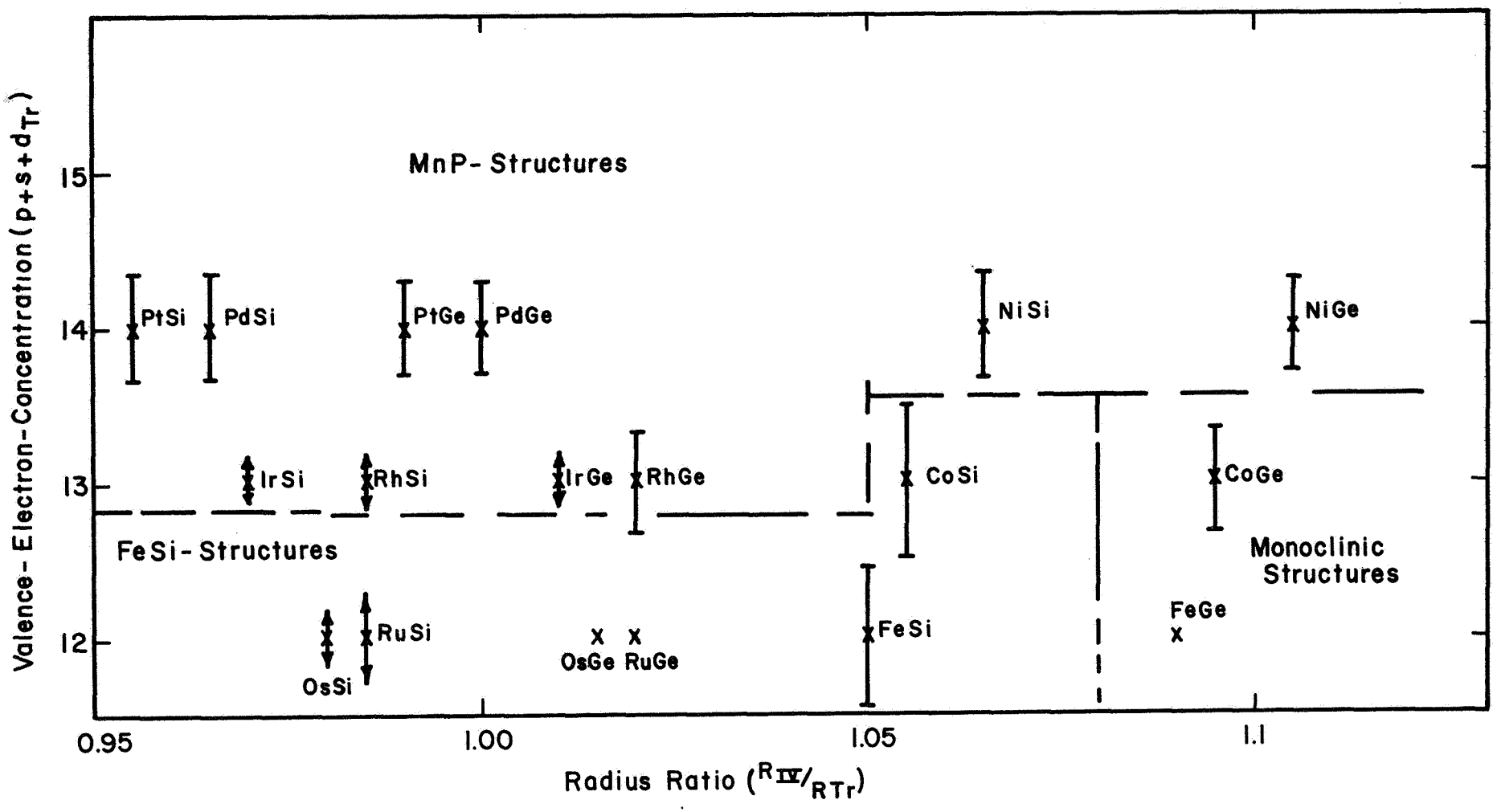

Fig. 10 Stability fields for group VIII silicides and germanides of VIII-IV stoichiometry.

x without bar = compounds not found or extremely unstable.

= Ratio of melting point of compound to melting point of metal. Ratio of 1 = 2 cm.

= Unknown melting point ratio.

As far as radius ratios and valence electron concentrations are concerned, it may be seen that iron, cobalt, and nickel silicides and germanides of X_2Y stoichiometry are rather size-sensitive but insensitive to valence electron concentration changes. This is evident from the fact that going from silicides to germanides a structural change is encountered, whereas all germanides have the same structure (NiAs-type) as do the existing silicides (anti-$PbCl_2$ structure).

Opposed to these so-called iron metals are the platinum metals. They are insensitive to radius ratio changes as is evidenced by the fact that silicides and germanides of metals with differing radius ratios have the same structure. However, a change in valence electron concentration causes a structural change. (Ru_2Si and Ir_2Ge are at present inexplicable exceptions among the X_2Y stoichiometries.) For the XY stoichiometries at lower valence electron concentrations [12] as compared to higher ones [13, 14], this statement is still true, but it seems that now valence electron concentration becomes much more determining. We already know that CoSi can tolerate about 2/3 of Ge without changing structure so that here the radius ratio may be changed up to 1.08 without a structural change. Further plots of this type will be presented in subsequent reports for other stoichiometries. After intermediate radius ratios and perhaps some intermediate valence electron concentrations from ternary system investigations can be inserted, it may be possible to get to some generalized picture about the alloy chemistry of systems of group VIII transition metals with Si and Ge.

Such a system not only would be desirable in the present context of thermoelectric bonding but would also contribute to the general understanding of silicides and germanides.

D. The MnTe-PbTe-SnTe System

As mentioned previously, further efforts on this system are being discontinued in line with concentration of the metallurgical investigations on metal-silicon-germanium systems. Plans were to study first the boundary systems PbTe-MnTe and SnTe-MnTe which had not been investigated at all. The SnTe-MnTe system, however, was never started due to the redirection of effort.

A preliminary phase diagram of the PbTe-MnTe system based solely on thermal analysis investigations and on preliminary studies of as-cast microstructures, was presented in the previous semi-annual report. It was quite clear that the phase relationships presented there merely reflect the substantial complexity of the situation. It was also speculated that in view of this complexity the strange precipitation phenomena observed in 3P material under a temperature gradient can at least be accepted as being due to the material itself.

Further investigations, notably by X-ray analysis, reveal some additional facts which show that the phase distribution as given in the previous diagram may not be correct. However, this does not detract from the fact that complicated precipitation sequences should be found in 3P material.

From the analysis of Debye-Scherrer photographs of specimens annealed for from 300 to 500 hours at 400 and 550°C, it becomes clear that the alloys are not in pseudobinary equilibrium. This is evident from the fact that $MnTe_2$ is found in the alloys and is also quite visible from lattice parameter vs. composition plots as shown in Fig. 11. Thus, the phase diagram presented in the Semiannual Phase Report No. 2 represents an arbitrary cut through a ternary system but not pseudobinary equilibrium. Some of the phase fields then must contain $MnTe_2$.

In principle, this condition might be due to loss of Mn by oxidation and thus constitute an experimental error. This possibility is discounted, however, since no significant MnO inclusions have been found in the microstructures. Also Fig. 11 would still be difficult to explain on the basis of such an experimental error.

Given the assumption that the SnTe-MnTe system shows a similar complexity (which is more than likely), it may still be concluded that the precipitation phenomena in 3P material arise from the fact that a metallurgically very complex system has to be used to produce desirable thermoelectric properties.

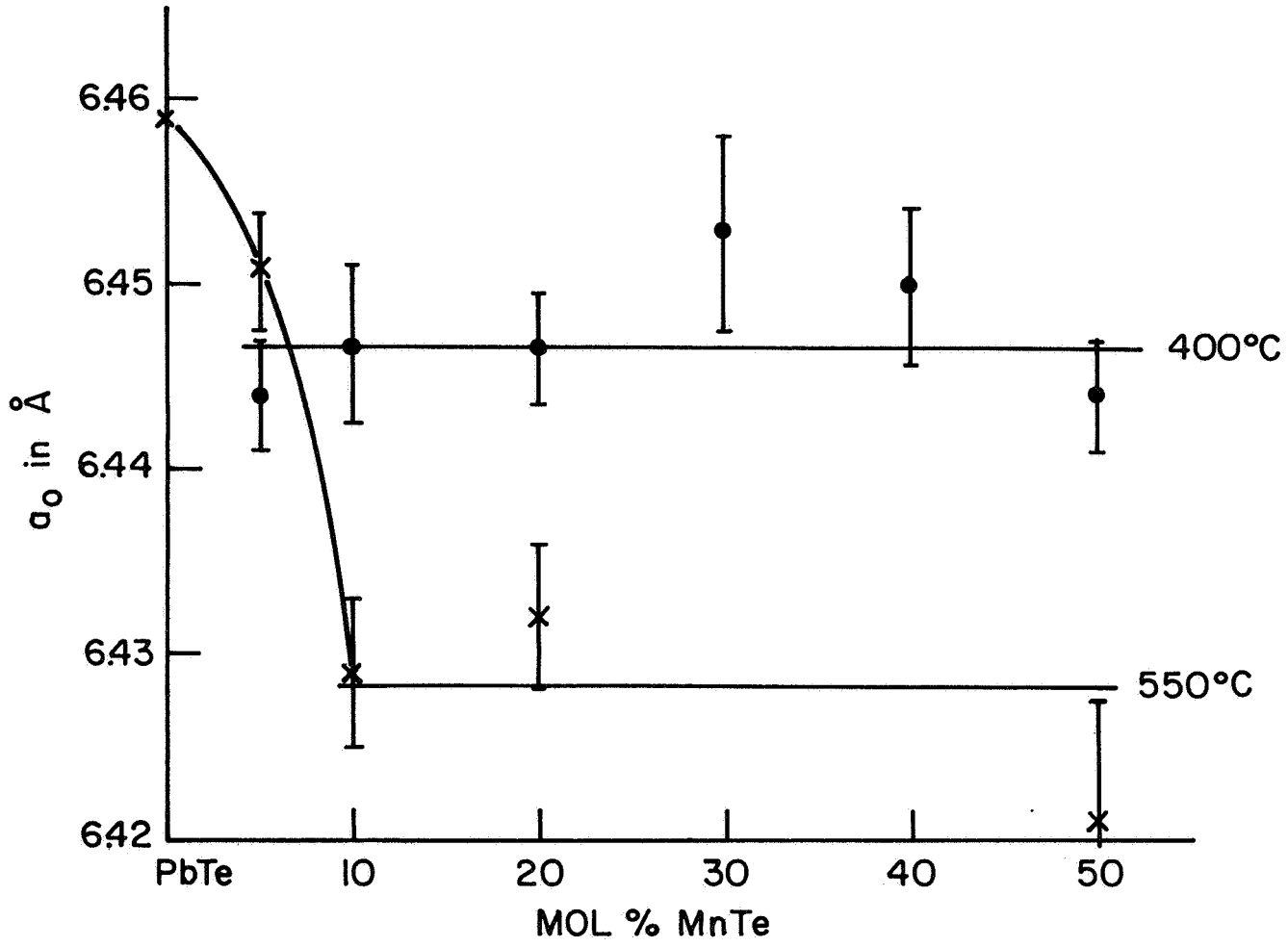

Fig. 11 Lattice parameter vs. concentration in sodium chloride type PbTe-MnTe solid solutions at 400° C and 550° C.

III. DESIGN OF SEGMENTED COUPLE MODULES

1. Synopsis

Design effort was directed at creating functional packaging for individual couples so that a module of any regular shape and any desired power output can be assembled in building block fashion, using only simple fastenings such as screws.

The thermoelectric building block or submodule will serve a dual function since it will inherently possess the characteristics of an ideal test bed for couples whose performance is to be evaluated. Any such evaluation of a couple will implicitly combine a live test of the submodule/building block hardware.

A final packaging concept has been arrived at after considering various approaches for insuring good thermal and electrical contacting from the couple to the surrounding package. Vital to this approach is the use of tiltable or "rocker" shoes presoldered to the couple. After incorporation into the support structure (module), the couple shoe interface is brought to a temperature at which loads on the "rocker" shoes applied by the pistons can readily deform the solder and allow the shoe and surface to be brought into a condition of "perfect" parallelism with the piston and, by inference, "perfect" contact with the electrical interconnecting strap separating the two.

This method has the virtue of eliminating very tight tolerances on the individual parts making up the total module structure. Stringent flatness need only be maintained on certain contacting metal surfaces, which is not generally an expensive operation.

2. Design Goals

The ultimate goal of this aspect of the program is to point the way to reliable, long-lived building block modules that will operate in a 1000/200°C regimen.

It is assumed that in the near future materials problems will be overcome, and it will be possible to fly generators working at these temperatures. Packaging for the modules will be designed with these goals in mind even though the segmented couples cannot operate at these temperatures right now. The testing of modules will be limited to the 800/50°C regimen that the couples are capable of and at whichthey have already been dimensionally optimized*.

3. Couples

The requirements for the silicon-germanium couples have been finalized and are incorporated in Dwg. No. 567-206, see Appendix.

The single American source for this material will not entertain an order as small as 20 couples or even 100 for that matter; thus overseas sources must be used. The best couple pricing is for a hot strap of high doped silicon and such couples have been ordered with the center distance between element legs reduced to a minimum, consistent with the design and fabrication of other parts of the module, to reduce overall size and cost.

The "D" shaped leg has not been faced inward to save space because this would require the use of a "D" shaped piston and cold shoe hole and would unnecessarily complicate the module.

4. Conceptual Design

A schematic building block is shown in Fig. 12 in which the cold end is the mounting surface and the hot end is left unsupported and free of encumberances. Thermal and electrical interconnections are complete at the "P" leg (most fragile) and the interconnecting "P" dumbell strap is ready for insertion into the adjoining module or a power take-off bus.

---

* Sixth Quarterly Report, Contract No. NAS 5-9149, covering period November 1966 - January 1967, p. 16.

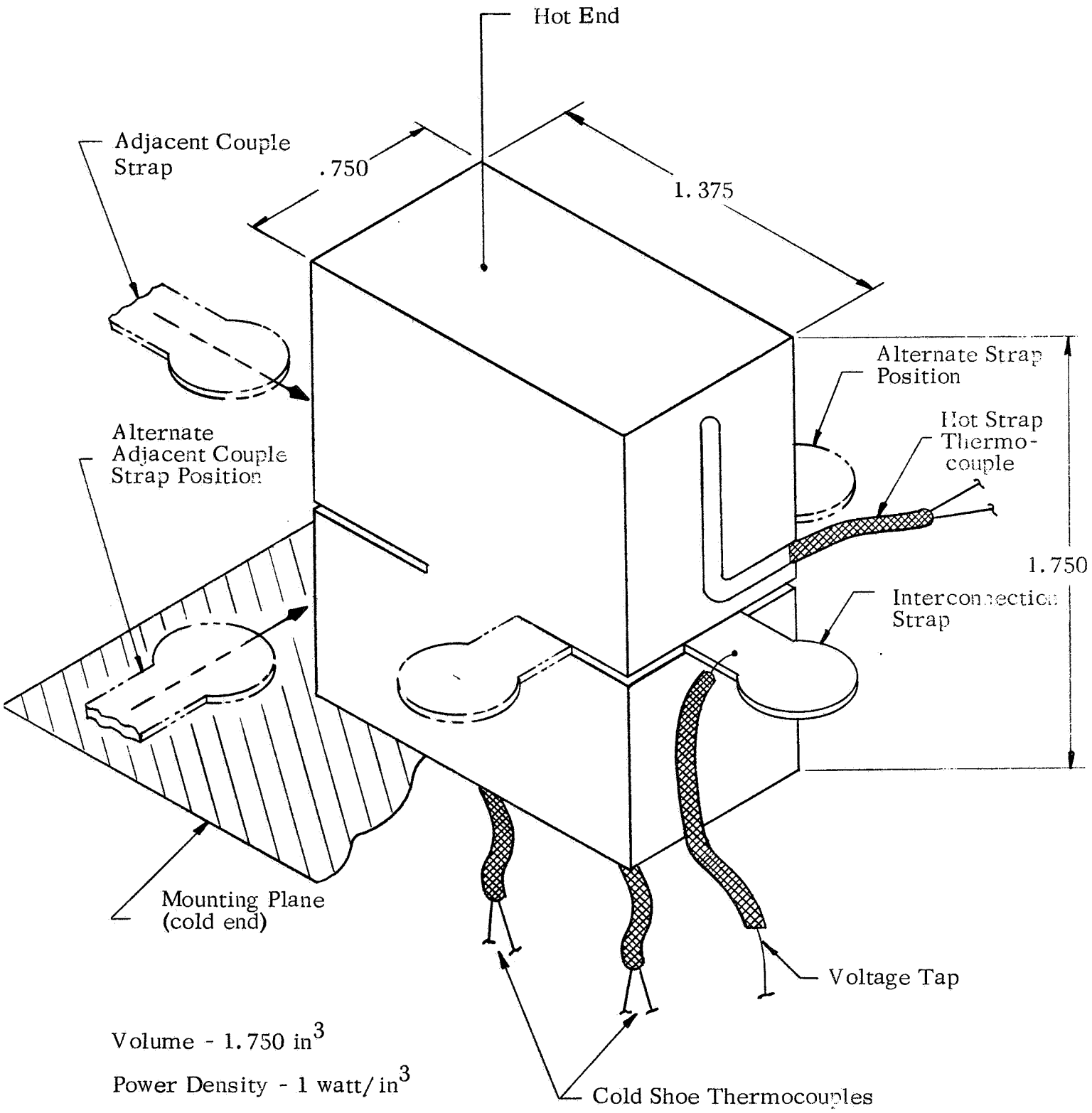

Fig. 12 Thermoelectric building block (sub-module) scale: 2/1.

When an interconnecting strap is inserted into the feedthrough slot at the N leg and the N leg piston loading applied by backing off a jacking screw, the entire unit is thermally and electrically placed in the circuit. Instrumentation probes as shown in the illustration provide hot and cold shoe temperatures in proximity to the couple and the couple output voltage.

The power density of an individual block is expected to be approximately one watt per cubic inch. Arrays of blocks into possible module configurations have been partially explored in Fig. 13, and except for the radial mountings, all use interconnecting straps that are identical.

For an individual block, the mounting concept that has evolved treats the segmented couple as an inherently frangible object. The large over-all dimensions of the couple and the 1000° C hot strap requirement generates pronounced expansibility. It is primarily for these reasons that bonded connections at the cold shoes are not being considered as a mounting possibility.

The system that will be used resembles some spring loaded piston designs employed by others, but some subtle differences exist in the degree of mechanical overload protection afforded the couple and the efficiency of heat conduction at the cold junction. The couple in essence "floats" within the constrainment provided by parallel surfaces (Fig. 14). The "floating" action is restrained only by frictional forces existing in the planes of the hot strap and the cold shoes where they abut the hot plate and the interconnecting straps, respectively.

The spring loaded piston supplies the normal forces at the shoe/strap interface for electrical and thermal conductivity and at the strap/piston interface for thermal conductivity.

The cold plate and pistons are hardcoated aluminum which enable very precise, non-sieze fits to be obtained between the two, provides electrical insulation and excellent thermal conductivity.

(1) Single row, long side, linear array (plan view).

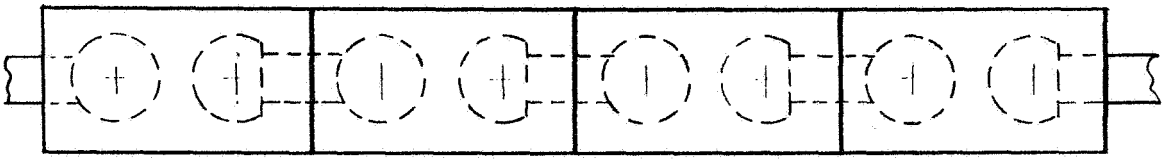

(2) Multiple row, long side, rectangular array (plan view).

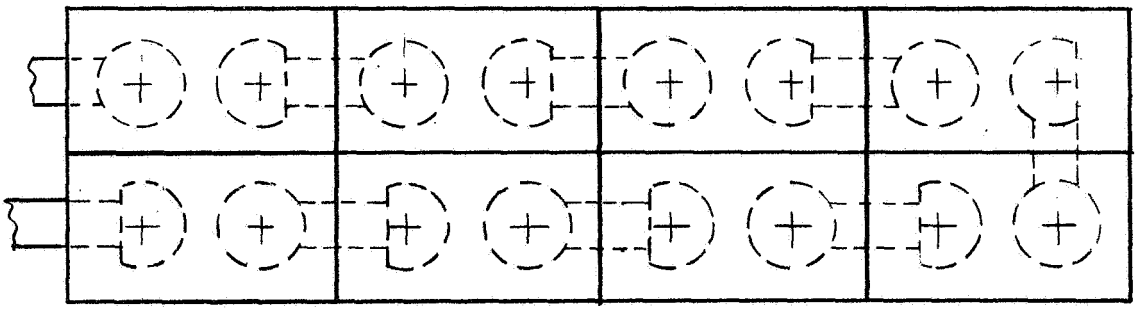

(3) Single row, short side, linear array (plan view).

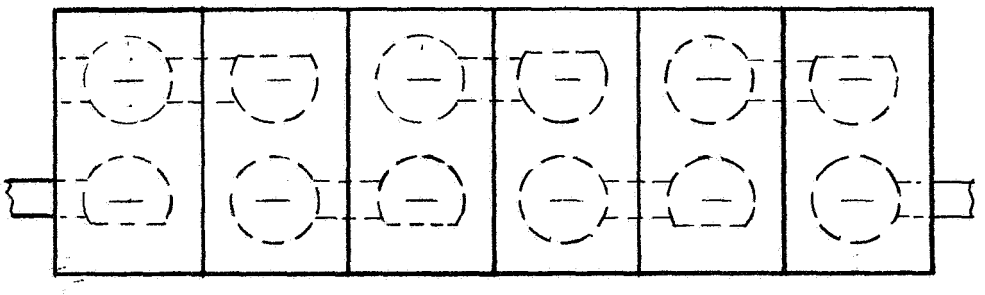

Fig. 13 Sub-module building block arrays.

(4) Multiple row, short side, rectangular array (plan view).

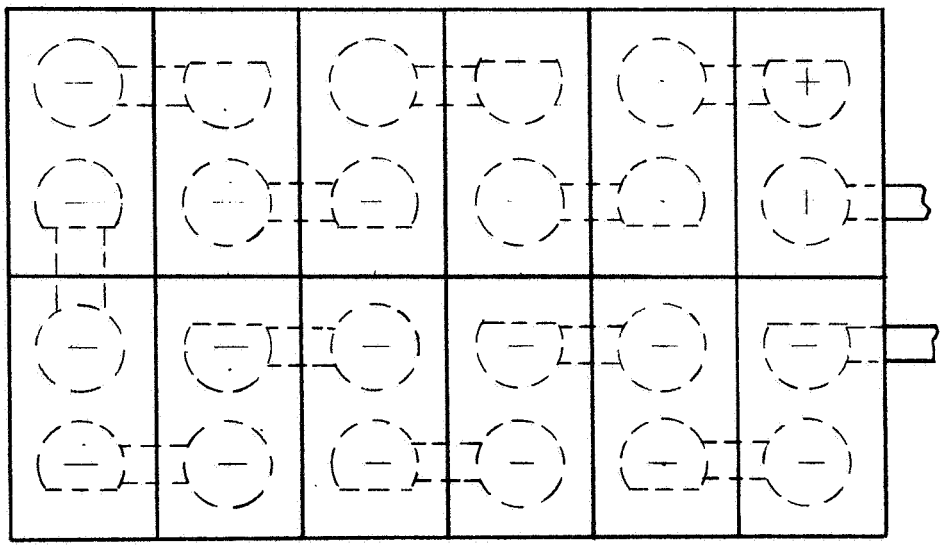

(5) L shaped linear array (plan view).

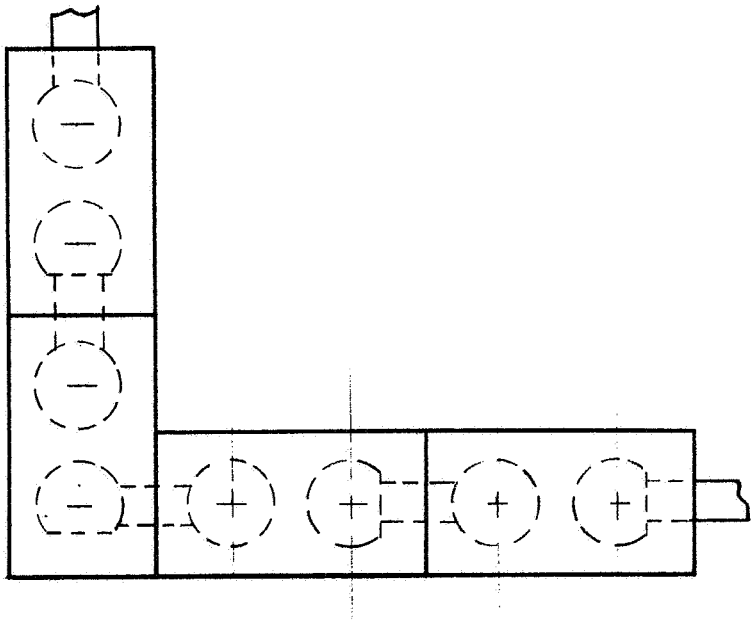

Fig. 13 (Cont.)

(6) Short side, radial array (end view).

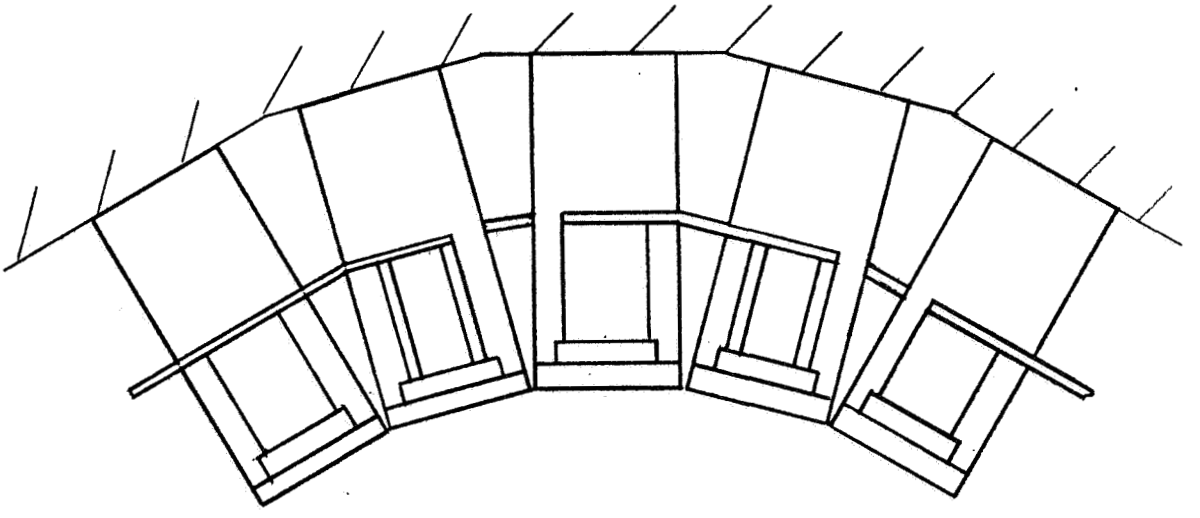

(7) Long side radial array.

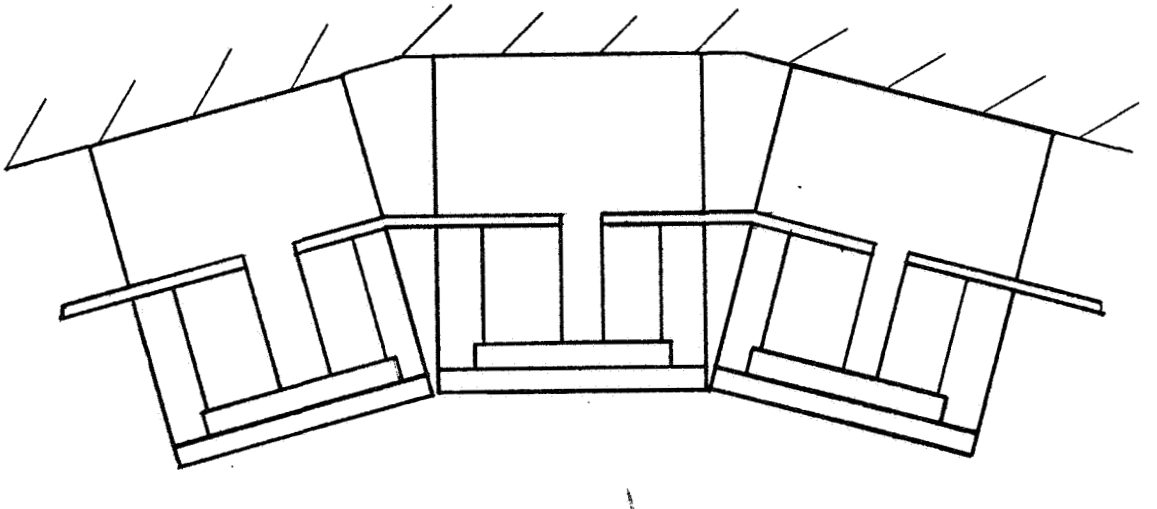

Fig. 13 (Cont.)

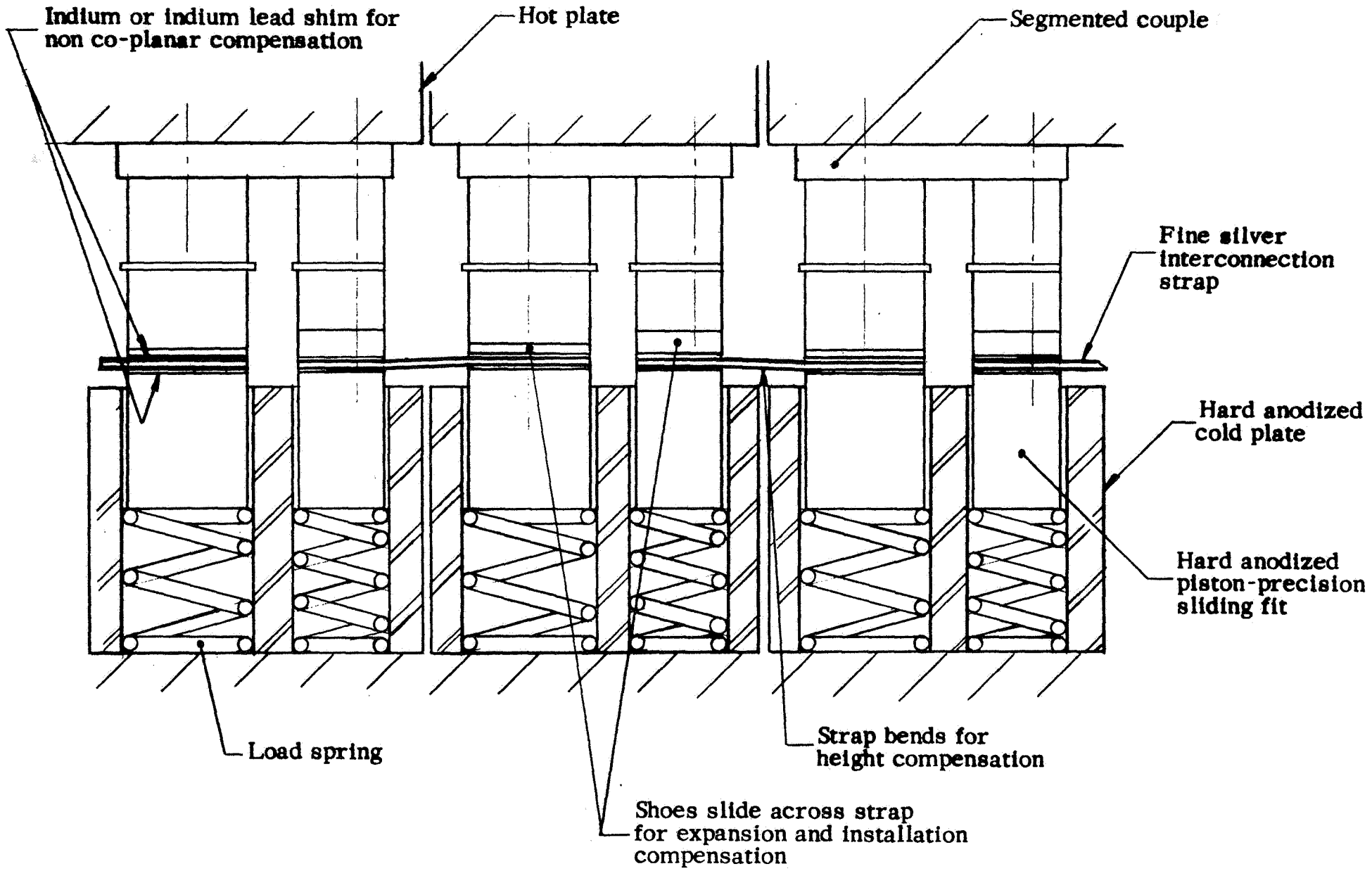

Fig. 14 Couple mounting concept (floating couples).

An inspection of Fig. 14 will reveal that the critical area is the interface between the cold shoe and the interconnecting strap. Any non-coplanar condition here will greatly reduce the contact area and profoundly affect joint resistivity (ohmic) and thermal conductivity. This is not as great a problem at the strap/piston interface since heat sink compounds can be used as fillers to compensate for minor misalignment. (In the interests of efficiency it is highly desirable to eliminate any buildup of filler which will suffer property losses due to radiation.)

The critical coplanar condition is almost impossible to achieve by care in fabricating and assembly alone, because small nonuniform dimensional changes in parts are bound to occur as the temperature of the structure is raised. Furthermore, the fragility of the couple and the sensitivity of lead telluride to foreign substances precludes virtually all known material removal methods for creating extreme parallelism between the hot strap and the cold shoes to begin with.

Therefore, the need for compensation at the interface becomes mandatory. One method being used to compensate for piston misalignment in thermoelectric modules* is a flat button that mates spherically with the piston and tilts to the required compensation angle with the shoe/strap. This approach suffers from a large temperature drop at the interface if the mating surfaces are not perfectly fitted. Indium foil has been used as an intermediate tolerance compensator to overcome this problem.

Another direction to take involves sweating tiltable "rocker" shoes to the couple in a fixture to obtain a high degree of parallelism and then using indium foil to enhance surface contact and compensate for only minor non-coplanar conditions.

Indium unfortunately melts at 154°C which is below the 200°C design goal for the package components. Also, the long-term properties of

---

* Snap-23A Program - Phase I, Thermoelectric Converter Development Program.

indium as an electrical contact element are not available and while its use as a purely thermal element seems sound, we are hesitant to insert foil or coat electrical contacts with the material.

If indium interfaced the piston/strap surfaces only, the shoe/strap interface gap could be completely shut if the piston loading were great enough to deform the strap the necessary amount, acting through the indium separator.

There is another approach which on paper at least seems the most promising. The couple again is fitted with "rocker" shoes pre-soldered but with no stringent parallelism specification applied. The finished couple is then installed in the module structure and inserted between a heater plate and cooler plate in the required atmosphere.

The module hot shoe may then be brought to 800° C and the cold shoe run hot enough to cause the couple "rocker" shoe interface to be readily deformable under the loading applied by the pistons. The result should be the creation of intimate "total" area contact* at the shoe/strap and strap/piston interfaces which is "locked" in, at lower actual operating temperatures. Long-term creep deformation or warping of the module structure would be compensated for by creep compensation in the "rocker" shoe joint.

---

* From "Basic Properties of Electric Contacts," Dr. J. B. P. Williamson, Electrical Contacts Proceedings of the Engineering Seminar on Electric Contact Phenomena.

"One of the chief characteristics of the surfaces of metals is their roughness; no matter how carefully they are prepared they always have irregularities. The nature of the contact between two solids is markedly influenced by the roughness of their boundaries. Whenever two metals are brought into contact, their surfaces touch first at those points where the asperities on one meet those on the other. The intense local pressure causes the metal in these tiny regions to deform. As the surfaces approach, the existing areas of contact grow and new areas are created as other asperities touch, until the total contact area is just sufficient to support the load. But even when this process is finished and considerable deformation has occurred, the major part of the surfaces will still be separated by distances which are very large compared with the range of atomic forces: the metals will be held apart except at a few small areas where true intimate contact occurs."

The only gray area in using this approach is that during hookup of the modules an "N" strap must be inserted into a "P" leg, as explained. The "parallelism burn in" operation for the module as described does not include compensation for the particular inserted strap. This could be a very minimal problem, however, because thickness uniformity is easily held to low "tenths" if desired and furthermore solder creep at the rocker joint will probably offset any strap effect in time.

To insure ideal starting parameters, however, a "parallelism burn in" could be performed prior to starting the testing of a group of interconnected modules.

5. Design

Complete drawings of the module, including an outline, assembly and details are presented in the Appendix. The details should not be considered completely finalized and have been set up to facilitate the heat transfer study and cost estimating.

The module components have been toleranced so that the .0045" maximum "rocker" compensation cannot be exceeded by the combined extreme dimensions at assembly.

Once a strength of materials and cost reduction study has been completed, the details will be reviewed and the module will be ready for fabrication.

The incorporation of thermocouples as an integral design element has proven to require too many design compromises and is being dropped. All modules, however, will be instrumented with couples and voltage taps as required for the testing phase by welding or cementing at required locations, and with mounting holes provided when necessary.

6. Process Fixturing

An assembly procedure for sweating shoes to couples has been established (Fig. 15) and a sweating fixture fabricated (Figs. 16a, b, and c). This method has already been tried on a good sampling of existing couples, with notably good results compared with previously used methods such as grinding and lapping.

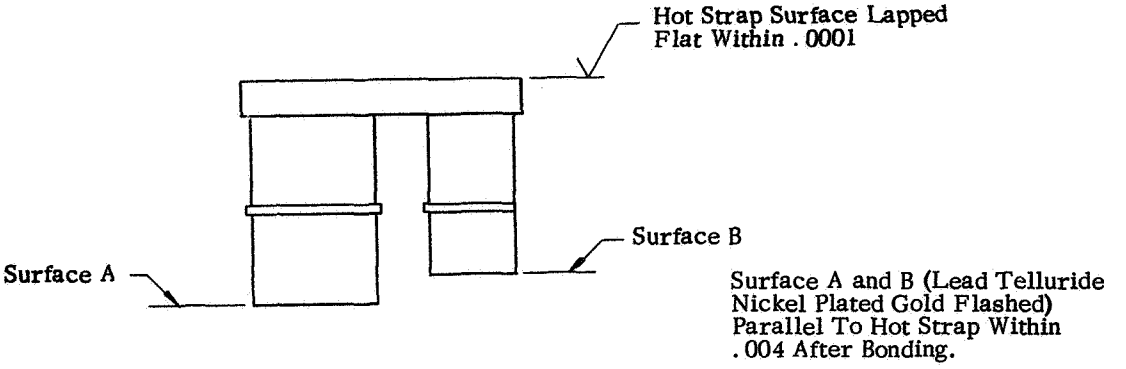

(1) Segmented Couple Less Shoes

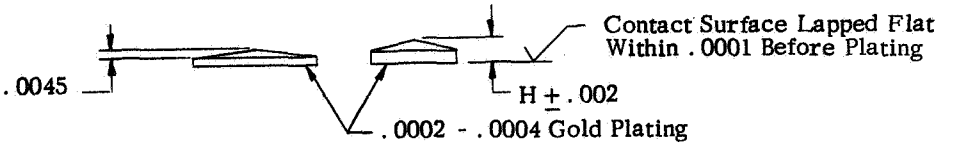

(2) Copper Shoes as Machined and Plated

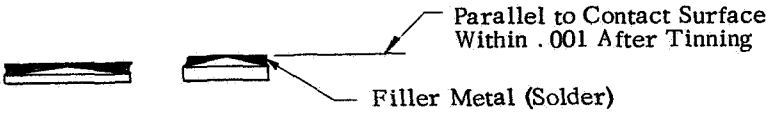

(3) Copper Shoes After "Tinning" In Fixture
No. 567-202

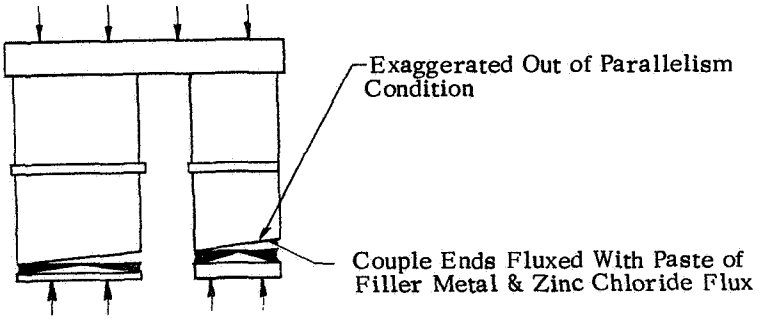

(4) Couple and Shoes Assembled in Fixture
No. 567-201

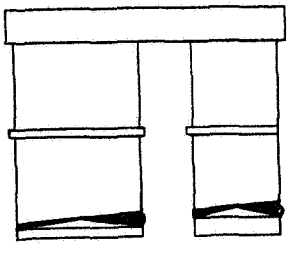

(5) Completed Unit-Hot Strap & Contact
Surfaces Parallel Within . 0002" - . 0005"

Fig. 15 Assembly stages in precision sweating of shoes to segmented couples.

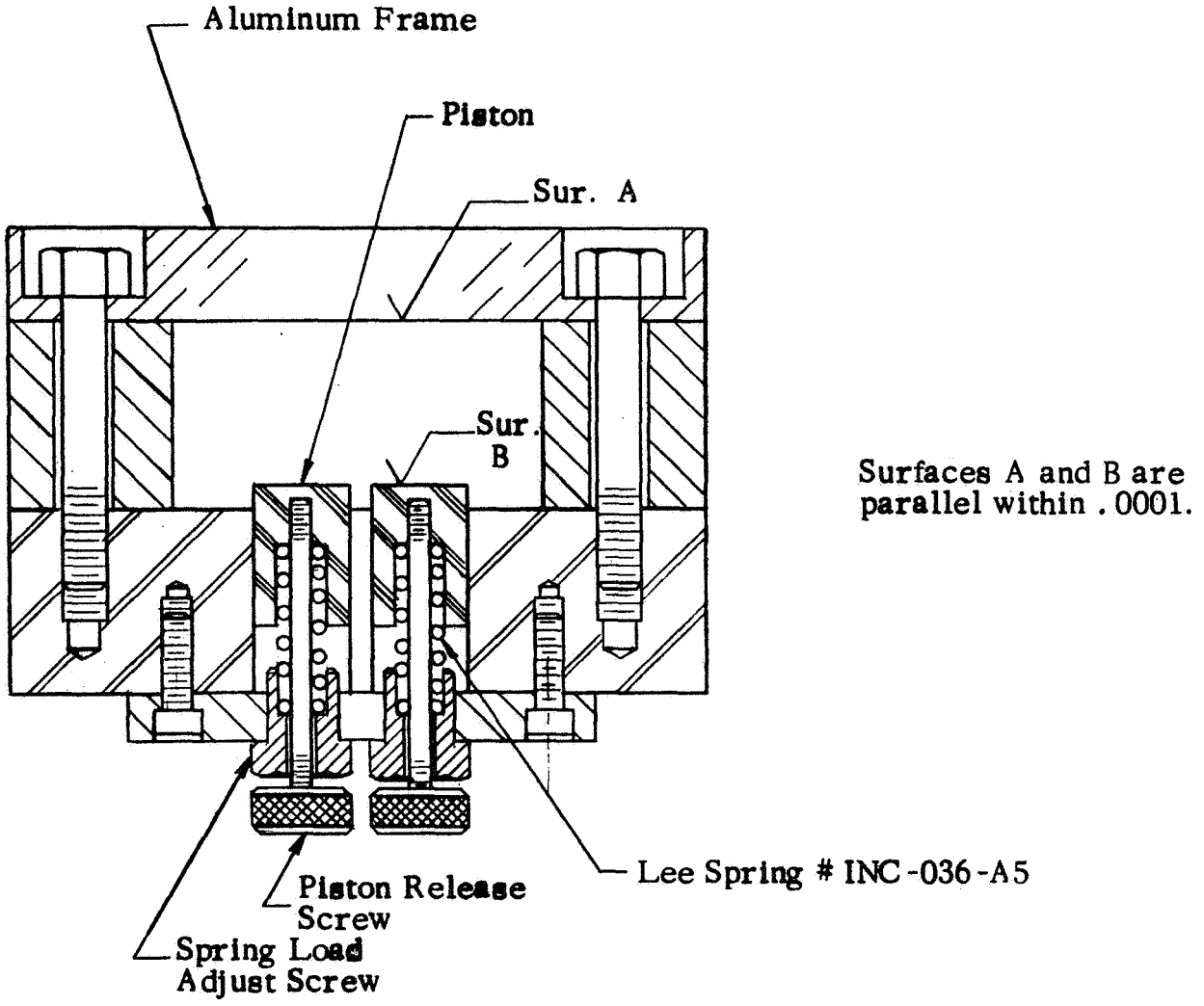

Fig. 16(a) Couple shoe sweating fixture no. 567-201.

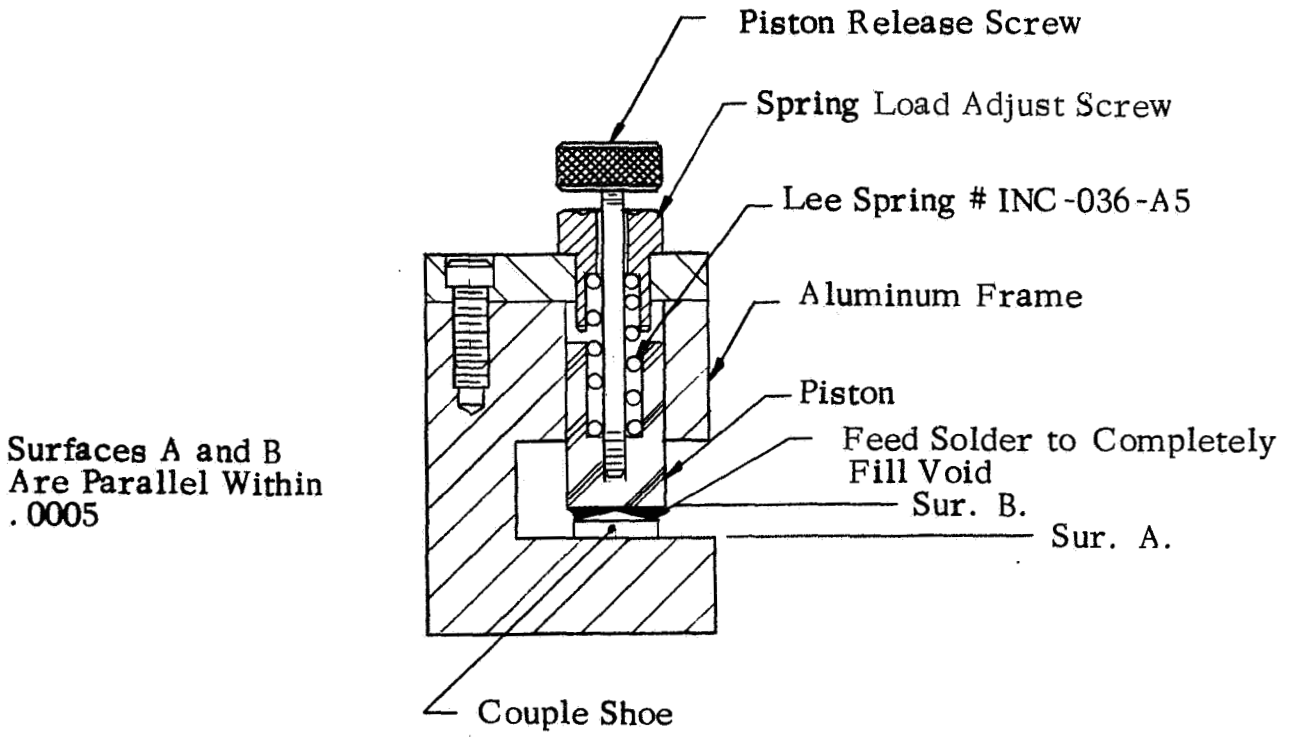

Fig. 16(b) Shoe tinning fixture no. 567-202.

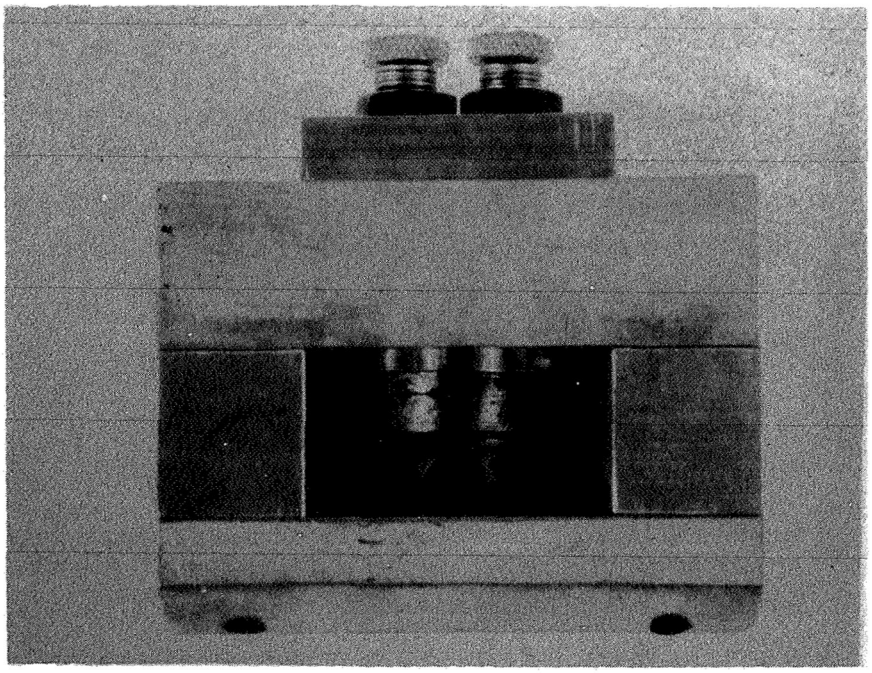

Fig. 16(c) Couple shoe sweating fixture (couple in place).

Couples that have been run with this method are checked on a CEJ "Microkator" that can reliably measure parallelism to 50 millionths of an inch. In those instances where reasonable care was taken and the prior dimensional characteristics of the couples were known, the parallelism of hot strap to shoe contact surface was typically .0005", with readings of .0002" not uncommon.

A solder with a melting point of 490°F was used, which is almost mandatory for a cold shoe operating temperature goal of 392°F. Some difficulty in debonding of the tungsten/lead telluride joint was experienced which may be a reflection of fixture (expansion) or materials (high melting point solder) problems. Since the couples themselves had been previously soldered and temperature cycled and may be defined as being "old" material, the problem cannot be resolved until new material is obtained.

The method of checking the soldering fixture itself on a surface plate is shown in Fig. 17. The fixture is clamped to an angle plate and surface "A" is located and indicated parallel to the surface plate. A gage block is then clamped against a piston face (surface "B") by interposing a ball between surface "A" and the block to insure perfect contact between the two. The portion of the gage block cantilevered beyond the fixture is then indicated using the "Microkator."

7. Heat Transfer

From the heat transfer viewpoint the design objective is to maintain the optimized steady state temperature gradient across the couple.

For a fixed heating and cooling capacity upon which the couple end temperatures are based and the couple geometry optimized, temperature drops caused by the thermal resistance of materials and contact interfaces in series with the couple lower the efficiency of the module (generator). The sizing of the heating and heat dissipation sources is based upon heat flow through the active portion of the module and the end temperature requirements plus heat shunt losses through the media

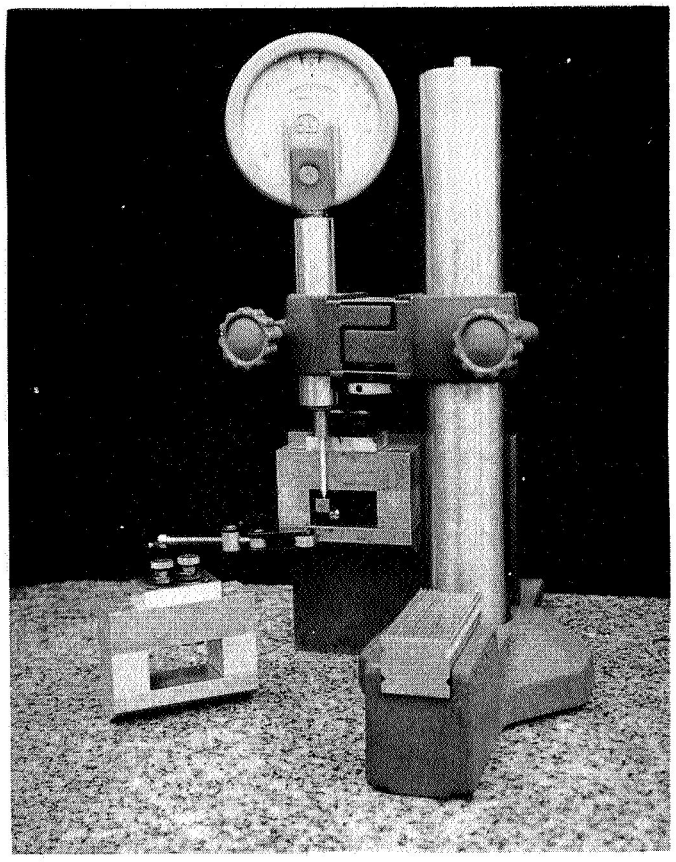

Fig. 17 Inspection procedure for checking the parallelism of surfaces "A" and "B" of the couple shoe sweating fixture.

(insulator), filling voids in the module structure and other purely structural members. There are other losses in an actual generator, but in order to maintain a proper focus there is no point in discussing these here.

The purpose of a heat transfer study, then, is to denote the actual expected temperature drops across the module and the heat shunt loss from hot to cold shoe. For simplicity, certain losses and material properties are being neglected. To illustrate, losses based on radiation, conduction and convection from the sides of the module are not being considered. Convection in certain natural voids in the module structure (strap area) is not being considered. The change in thermal conductivity of materials as a function of temperature gradient is being neglected and a mean K used.

T he theoretical thermal input previously determined at the 800/50° C optimization temperatures is 29. 4 watts. This heat flow is divided equally between the couple legs.

Neglecting edge losses or assuming heat flows only perpendicular to the surfaces, the heat flow across each side of the module is 14. 7 watts, since the same amount of heat must flow through each layer of material and across each interface.

$$q = \frac{A\, k_m\, (t_1 - t_2)}{x} = 14.7 \text{ watts} \times \frac{3.412 \text{ btu/hr}}{\text{watt}} = 50 \text{ btu/hr.}$$

where

A = area in ft^2 perpendicular to the direction of flow

km = mean thermal conductivity btu/(hr) (sq. ft.) (day F/ft.)

$t_1 - t_2$ = temperature differences, deg. F.

q = steady state heat flow.

Working from the SiGe couple hot end (a) 800° C (1472° F), three layers of material are encountered: the high doped silicon bridge, the alumina insulator, and the molybdenum hot shoe. Because of the relatively

high temperatures, radiation is effective enough to cancel contact resistances at the material interfaces. Therefore the required temperature at the hot shoe outer surface is calculated using the equation above and referring to Fig. 18 for subscript denotation.

High Doped (approx. 10^{19} Carrier Concentration) Silicon Hot Strap

t_6 = 1472°F (given) at SiGe end surface

from Dwg. no. 567-201-1 (see Appendix), SiGe-PbTe Segmented Couple

$$A = \frac{.480'' \times .852'' \times}{144} = .00284 \text{ ft}^2$$

$$x = \frac{.125''}{12} = .00108 \text{ ft}$$

k at 1472°F = 19.35 btu/(hr)(ft^2)(deg F/ft)

$$t_5 = \frac{qx}{Ak} + t_6 = \frac{50\ (.00108)}{.00284\ (19.35)} + 1472$$

t_5 = 1473°F

Compression Interface ($t_4 = t_5$ assumed).

High Alumina Insulator

t_4 = 1473°F at Silicon hot strap surface

from Dwg. no. 567-213 (see Appendix), Insulator

$A = .00284 \text{ ft}^2$

$$x = \frac{.010''}{12} = .000834 \text{ ft}$$

k at 1472°F = 70

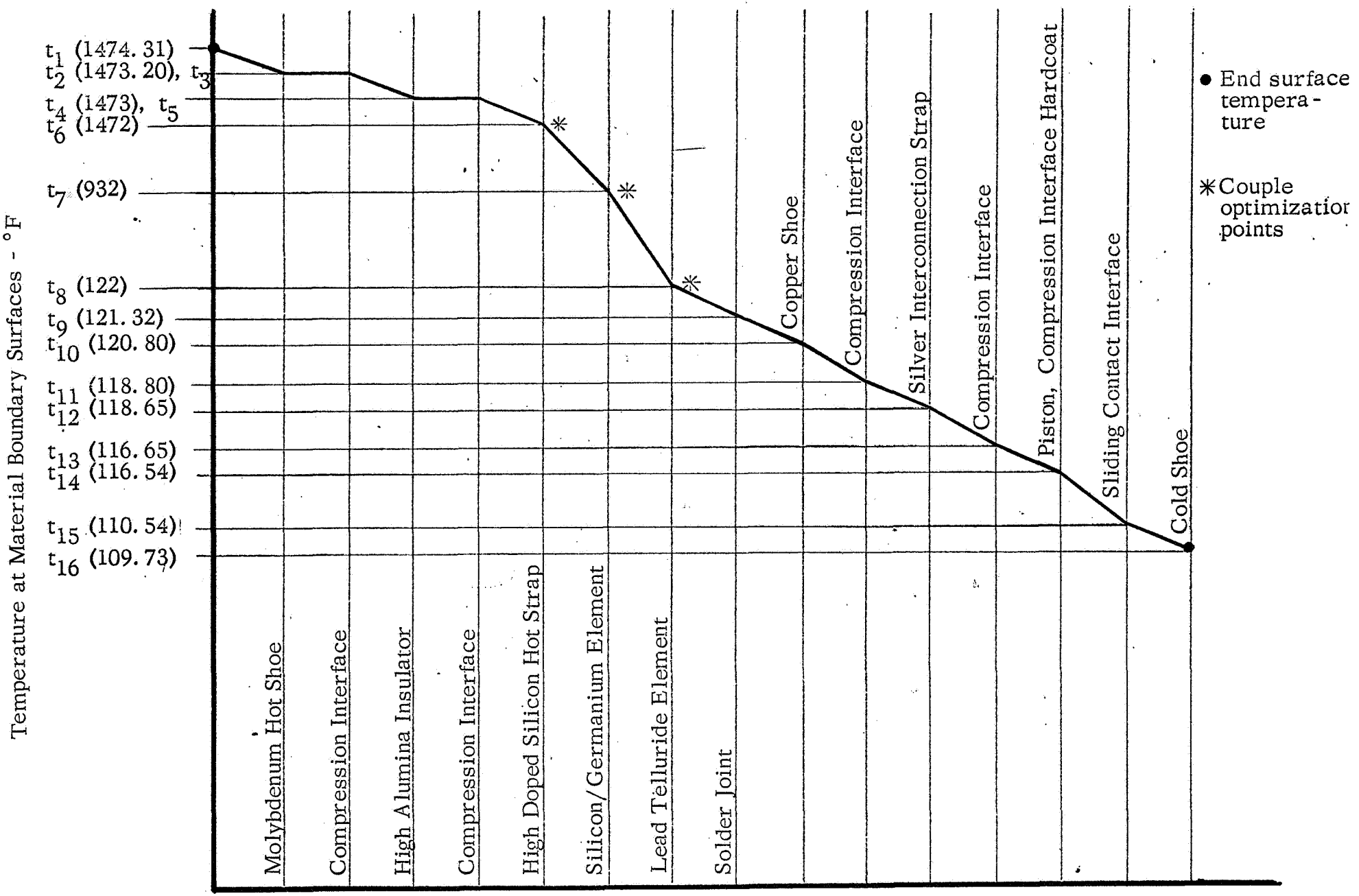

Fig. 18 Steady state temperature differentials within module.

$$t_3 = \frac{50\,(.000834)}{.00284\,(70)} + 1473$$

$$t_3 = 1473.2°F$$

Compression Interface ($t_2 = t_3$ assumed)

Molybdenum Hot Shoe

t_2 = 1473.2 at alumina insulator surface
from Dwg. no. 567-207 (see Appendix), Hot Shoe

$A = .00284\ ft^2$

$$x = \frac{.062"}{12} = .00517\ ft$$

k at 1832°F = 82.2

$$t_1 = \frac{50\,(.00517)}{100284(82.2)} + 1473.2$$

t_1 = 1474.31°F (would be 11° higher if nickel based alloys with a conductivity 1/10 of molybdenum were used).

Working from the SiGe hot end toward the cold shoe of the "N" leg

t_7 = 932°F at Tungsten Bond
t_8 = 122°F at Lead Telluride end
} by previous optimization.

Solder Joint ("N" leg)

t_8 = 122°F at Lead Telluride end surface
from Dwg. no. 567-203 (see Appendix), Element,
Lead Telluride 3N

$$A = \frac{.150}{144} = .0015 \text{ ft}^2$$ (Solder joint dram. same as lead telluride dram.)

$$x = \frac{.0045"}{12} = .000375 \text{ ft}$$ (actually only 1/2 joint volume is solder, rest copper)

$k = 19.6$ (assume pure lead)

$$t_9 = t_8 - \frac{qx}{Ak} = 122 - \frac{50\,(.000375)}{.00115\,(19.6)}$$

$t_9 = 121.32°F$

Gold Plated Copper Shoe

$t_9 = 121.32°F$ at solder joint surface

from Dwg. no. 567-203 (see Appendix), Shoe, type N

$A = .00115 \text{ ft}^2$

$x = .032"/12 = .00266 \text{ ft}$

$K = 226$

$$t_{10} = 121.32 - \frac{50\,(.00266)}{.00115\,(226)}$$

$t_{10} = 120.80°F$

Compression Interface

A 2°F temperature drop will be assumed setting $t_{11} = 118.80°F$

Silver Interconnection Strap

$t_{11} = 118.80$ at show interface

from Dwg. no. 567-212, see Appendix, Strap, Interconnection

$A = .00115\ ft^2$

$x = .010"/12 = .000834\ ft$

$k = 242$

$$t_{12} = 118.80 - \frac{50\ (.000834)}{.00115\ (242)}$$

$t_{12} = 118.65°F$

Compression Interface

A 2°F temperature drop will be assumed setting $t_{13} = 116.65°F$

Piston, Compression Interface Hardcoat

$t_{13} = 116.65°F$ at strap interface

from Dwg. no. 567-209 (see Appendix), Piston

$A = .00115\ ft^2$

$x = .0023"/12 = .000191\ ft$

$k = 70$ (85% dense Al_2O_3 at 300°C)

$$t_{14} = 116.65 - \frac{50\ (.000191)}{.00115\ (70)}$$

$t_{14} = 116.54°F$

Sliding Interface (Piston/Cold Shoe)

A uniform heat distribution from the top of the piston into the surrounding cold shoe will be assumed and the hard coat/sliding interface drop taken as 6°F setting $t_{15} = 110.54°F$.

Cold Shoe

$t_{15} = 110.54°F$

from Dwg. no. 567-208 (see Appendix), Cold Shoe

$A = .03835\ ft^2$ (1/2 of surface B minus .437 hole)

$x = .750"/12 = .0625\ ft$

$k = 111$

$$t_{16} = 110.54°F - \frac{50\ (.0625)}{.03835\ (111)}$$

$t_{16} = 109.73°F$

Cold Shoe Hardcoat

Temperature drop is negligible.

Conclusion

The calculated temperatures at the hot and cold shoe surfaces are 1474.31 and 109.73°F respectively to yield optimization temperatures of 1472 and 122°F at the couple hot and cold junctions respectively.

Heat Shunt Loss

Voids in the module structure are packed or filled with insulating material to prevent heat transfer from hot to cold shoe by radiative or conductive means.

In proximity to the hot shoe, Johns-Manville Micro-Quartz felt is used because it can be packed into the somewhat complex void area around the couple hot strap. At the point where the Micro-Quartz terminates, a molded piece of insulation is simpler to use and forms natural end walls for the module. Johns-Manville MIN-K is used for the block insulator and the 1000°C (1832°F) hotstrap requirement is just met by MIN-K 2000 which has a maximum service temperature of 1800°F.

Since the block insulator is not in contact with the cold shoe by virtue of item 16, Dwg. 567-206, see Appendix, Spacer, shunt heat is not passed from the block insulator to the cold shoe by conduction. However, the ceramic side support plates (item 5, Dwg. 567-210, see Appendix), do pass shunt heat because they are radiatively heated at the hot side and in intimate contact with the cold shoe.

Side Plate Shunt Heat Flow

$$q = \frac{Ak_m (t_{hot} - t_{cold})}{x}$$

from Dwg. no. 567-210 (see Appendix), Plate, Side

$A = .00019$ ft (slots and holes disregarded)

$x = .970"/12 = .087$ ft

$k = 29$ (conservative-value at 300°C for Steatite)

$q = .00019 (1832-110)/.087 = 3.76$ Btu/hr (single side)

Shunt, $q_{total} = 7.52$ Btu/hr.

IV. ISOTHERMAL LIFE TESTING

A large group of bonded 3P and 3N elements and unbonded 2P and 3P elements were put on test at 525°C on June 19, 1968.

All the elements in this group were taken off test after 1100 hours; those listed in Table I were measured for the first time at this point. The starting resistances of the remaining elements are listed in Table II.

The elements measured at 1100 hours were then re-encapsulated and the entire group was put back on test for 2000 hours. A number of new elements were also included at this time, and Ar-5% H_2 was used as the atmosphere for a greater number of elements. Table II lists the starting resistances and prior testing time of the elements put on test at this point.

There were several power interruptions during the second part of this test, ranging from a few minutes to three hours duration. It is felt that the resultant temperature cycles contributed substantially to the poor general performance of the elements. In addition, two of three furnaces which held the encapsulated elements, overheated to > 700°C during the initial cool-down period because of faulty controllers. Table III is grouped according to the three furnaces, with the first two groups corresponding to the overheated furnaces.

While the performance of most of the elements tested appears rather poor in terms of the number of surviving bonds, there are some interesting observations to be made. Twenty-two 3P-W contacts were tested; these had varying amounts of previous testing. At the end of this test, two 3P-W contacts were measurable; ten had failed, that is the contact simply came apart; and ten contacts were still intact, but fracture of their element made it impossible to measure their resistance. Some of these contacts are shown in Fig. 19. A number of these broken element-contact samples have withstood substantial periods of testing and only fractured during the temperature cycling of this test. One contact has remained intact, with its element, for over 10,000 hours. The initial

TABLE I

Resistance Values of Isothermally Tested Elements
Initial and 1100 hours

Element	0 hours (6/19/69)			1100 hours		
	CR_T $\mu\Omega$	CR_B $\mu\Omega$	Element mΩ	CR_T $\mu\Omega$	CR_B $\mu\Omega$	Element m Ω
6A1P24*	170	---	1.48	125	---	1.82
6A4P24*	150	200	1.60	145	200	1.655
6A6P24	150	---	1.45	160	---	1.79
6L2P30	---	160	2.04	---	250	1.80
6L5P30*	---	400	1.70	---	470	1.78
4P' 16	---	---	0.90	---	---	0.66
5P' 16	---	---	0.95	---	---	1.00
11P' 16	---	---	0.85	---	---	0.95
14P' 16	---	---	0.88	---	---	0.71
5R3N22	---	120	.530	---	---	0.500
5R6N22	---	200	.62	---	900	.500
5R7N22	100	70	.590	200	---	.600
5R8N22	---	95	.61	---	150	.530
5R9N22	100	120	.630	30	50	.670
5R10N22	---	95	.565	---	700	.500
5R12N22	70	60	.630	85	30	.555
5R14N22	75	120	.605	200	450	.510
5R13N22	85	60	.735	95	55	.750

* H_2-Ar atmosphere

TABLE II

Initial Resistances of Elements with Prior Testing
(as of 6/19/68)

Element	CR_{top} $\mu\Omega$	CR_{bottom} $\mu\Omega$	Element mΩ	Total Testing hrs.
31P37			2.30	1700
34P37			2.40	1700
35P37			2.35	1700
3P33A			2.60	1700
4P33A			2.45	1700
5P33A			2.20	1700
1P25			2.20	7300
2P25			2.20	7300
7H17P33A	---	130	1.87	1700
7I5P37	170	---	1.78	1700
7I9P37	---	120	2.21	1700
5D4P19	340	---	1.71	6000
5D7P19	375	---	1.88	6000
7I14P37	145	130	1.93	1700
6L4P30	---	120	1.97	7300
6I1P15	---	130		7300
6M6P24	230	100	2.12	7300
6M1P30		140	2.10	7300
5C3P19	---	180	1.80	6000
6M3P30	---	200	1.95	7300
7J2P37	270	175	2.16	1700

TABLE III

Room Temperature Resistance of Elements Tested
Isothermally for 3100 Hours

Element	CR_{top} $\mu\Omega$	CR_{bottom} $\mu\Omega$	Element m Ω	Total Testing hrs
5R13N22*	---	75	0.620	3100
5R9N22	300	100	0.603	3100
5R8N22*	200	700	0.580	3100
5R12N22*	---	70	0.530	3100
5R6N22	---	--	0.470	3100
5R3N22	---	--	0.540	3100
5R7N22*	---	--	0.480	3100
6L2P30	---	--	1.25	3100
6A1P24	---	--	1.50	3100
6A4P24	---	--	1.42	3100
34P37			2.32	4500
5D4P19	x	--	x	9100
7I7P37	---	--	x	4800
6L4P30*	---	--	2.05	10400
7J2P37	---	400	2.45	3100
6I1P15	---	240	x	10400
7I14P37*	---	x	x	4800
6M2P30	---	x	x	10400
5D7P19*		--	1.60	9100

TABLE III (Cont.)

Element	CR_{top}	CR_{bottom}	Element	Total Testing
7I5P37	---	x	x	4800
7I9P37	x	x	x	4800
3P33A*			2.25	4800
4P33A			1.95	4800
5P33A*			2.25	4800
1P25			1.90	10400
2P25*			2.75	10400
31P37*			2.05	4800
35P37			1.98	4800
6A6P24	---	---	1.65	3100
5R14N22	---	---	0.52	3100
6M6P30*	---	x	x	9400
6M1P30	x	---	x	9400
7H17P33A*	---	x	x	4800
5C3P19	---	---	x	9100
6M3P30*	---	x	x	9400

* H_2-Ar atmosphere

x Element fractured, making contact resistance measurement impossible, but contact still intact.

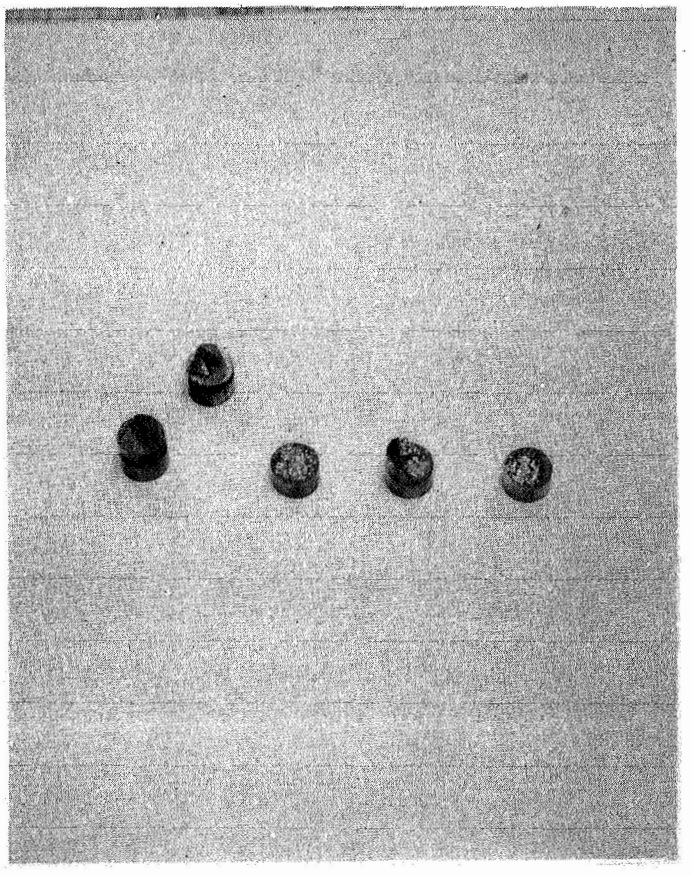

Fig. 19 3P-W contacts showing material bonded to W after fracture of elements. Time at 525°C test temperature varies from 9100 to 10, 400 hours.

resistance of the bottom contact to 6I1P15 was 75 $\mu\Omega$ and the element resistance was 1. 83 mΩ. Five of the broken contacts have been tested for 9100 and 9400 hours; however, it may be argued that the bond has been preserved by the relief of the stress due to the element by the element's having broken. This cannot be asserted positively either way, without the possibility of identifying a bond material or region.

V. FEASIBILITY OF USING CESIUM PLASMA LAMPS AS HIGH TEMPERATURE TEST SOURCES

We have undertaken to study the feasibility of using cesium plasma devices as high temperature (> 1000°C) heat sources for life testing of Si-Ge thermoelectric generators. Because of difficulties experienced with most of the existing heat sources, it was felt that a small effort which could lead to the definition of an alternate heater would be desirable.

A preliminary design for a prototype cesium-xenon plasma heater has been decided upon. The materials technology for construction of this device is based on development results for thermionic diodes operating as high as 1500°C, while the general configuration and operating parameters are based on alkali metal vapor lamp developments. The preliminary design is shown in Fig. 20.

The selection of materials for incorporation in this device was based on the results of a thorough study by the Nuclear Thermionic Power Operation of the General Electric Company[8]. This study dealt with the stability of various metals, ceramic metallizing coatings, and metal-to-metal joining techniques in conjunction with Lucalox and high purity polycrystalline alumina in vacuum and 20 mm of cesium vapor at 1250° and 1500°C. Lucalox bears a sufficient resemblance to the single crystal sapphire produced by Tyco's Special Products Division which will be used in fabricating these heaters, that it is felt the results obtained on Lucalox will be applicable to our material.

Columbium was selected as the "structural" metal, in contact with cesium, because of its excellent resistance to attack by cesium vapor and its almost perfect match in expansion coefficient with sapphire. Molybdenum was chosen for the electrodes for its high work function, resistance to cesium attack, and reasonable match with columbium in expansion coefficient.

A large class of metal-ceramic seals are made by first applying a metal coating to the ceramic and then joining the metal coating to metal structural members by conventional techniques of brazing or diffusion-

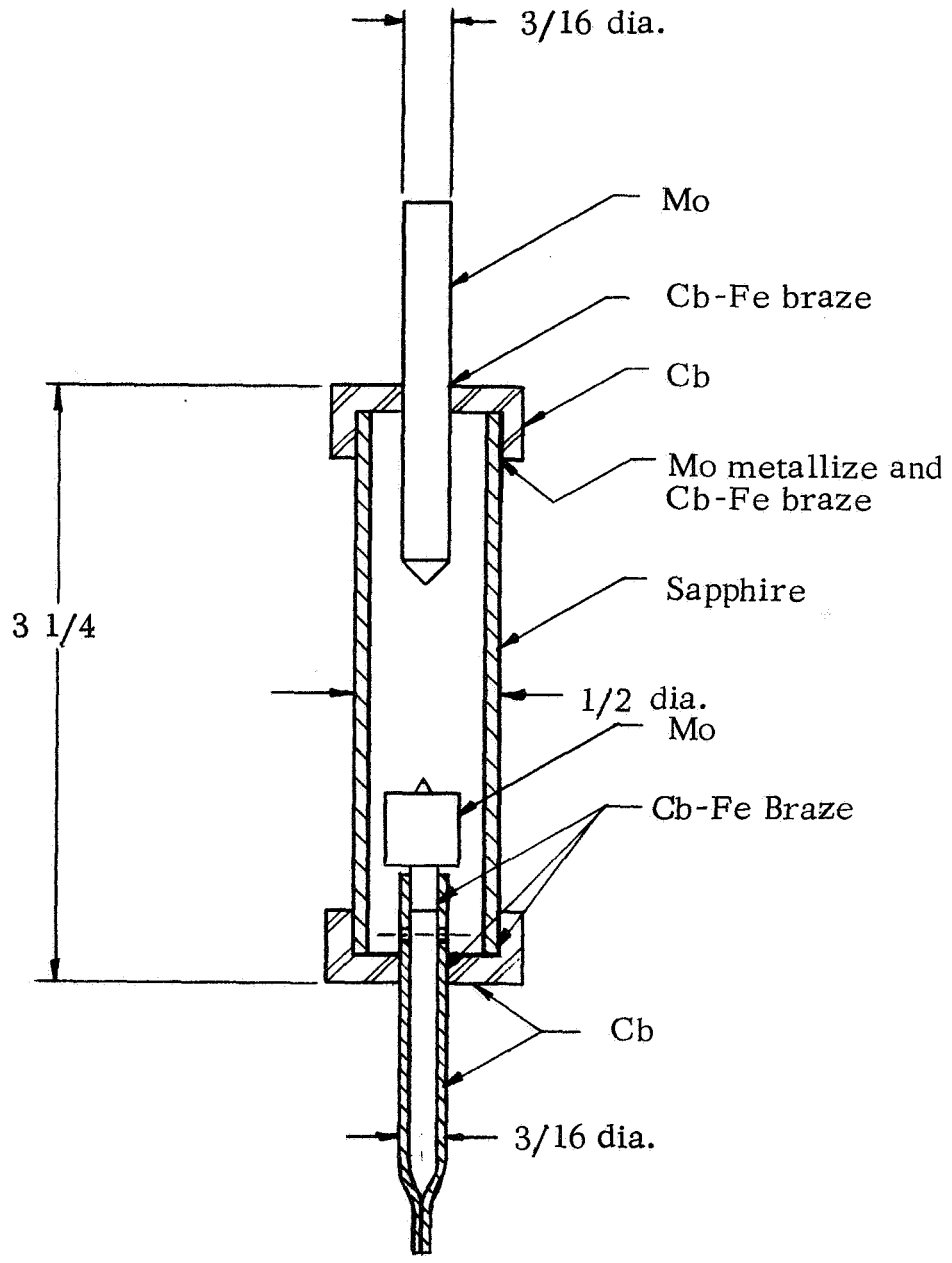

Fig. 20 Schematic cross section of preliminary design for cesium plasma heater.

bonding. In this case we have decided upon using a tungsten and molybdenum metallizing coating, containing additions of Al_2O_3 and Y_2O_3 to promote adhesion. A braze of 67 wt % Cb - 33 wt % Fe will be used for all joints in the structure. This braze, requiring a brazing temperature of 1670° C, has been shown to give good results in vacuum and Cs vapor testing at 1500° C[8].

Based on the operating parameters of cesium-xenon short arc lamps, we expect that the prototype will operate effectively with an input of approximately 20 volts at 10 amps. This is assuming operating pressures of approximately 0. 3 and 3 atmospheres for cesium and xenon, respectively.

Since it is to be expected that the entire device will operate at temperatures in excess of 1000° C, it is obvious that either vacuum or inert atmosphere must be provided to protect the metal portions from oxidation. In fact, it is even conceivable that an outer sapphire sheath could be provided to allow operation of such a device in air. With the inclusion of radiation shields the feed-throughs of the outer sheath could be kept at a low enough temperature to prevent harmful oxidation.

VI. REFERENCES

1. U. S. Patent no. 3,342,646, September 1967, A. G. F. Dingwall to Radio Corporation of America.

2. M. Hansen, Constitution of Binary Alloys, MacGraw-Hill, New York, 1958.

3. R. P. Elliot, Constitution of Binary Alloys, First Supplement, MacGraw-Hill, New York, 1965.

4. K. Anderko and K. Schubert, Zeitschr. Metallkunde 44, 307 (1953).

5. K. Schubert, K. Frank, R. Gohle, A. Maldonado, H. G. Meissner, A. Raman and W. Rossteutscher, Naturwissenschaften 50 (2) 41 (1963).

6. H. Pfisterer and K. Schubert, Zeitschr. Metallkunde 41, 358 (1950).

7. P. D. Garn, Thermoanalytical Methods of Investigation, Academic Press, New York, 1965.

8. Final Report, Contract No. NObs-90496, General Electric Company, July 1968.

APPENDIX

Thermoelectric Building Block Drawings

REVISIONS				
SYM	ZONE	DESCRIPTION	DATE	APPROVED

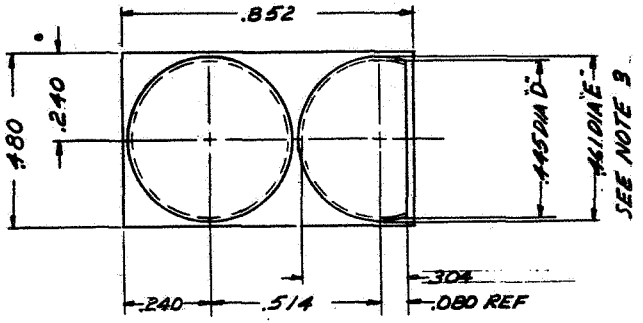

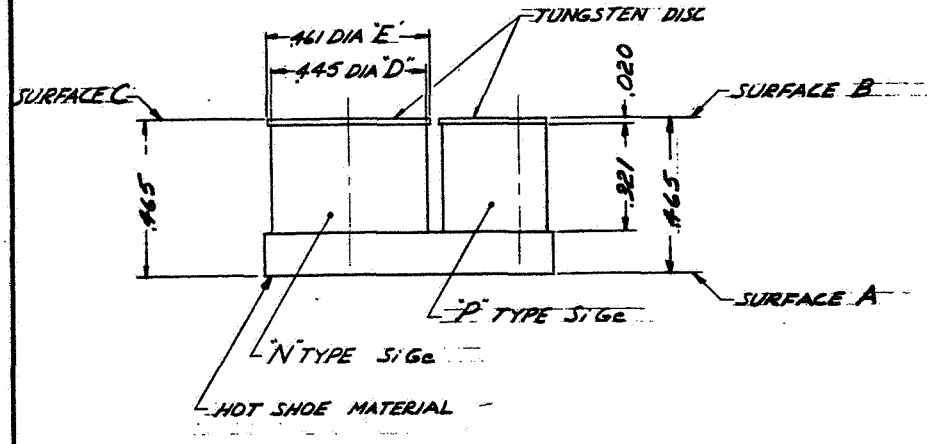

NOTES:
1. SURFACE A TO BE FLAT WITHIN .001"
2. SURFACE B & C TO BE PARALLEL TO SURFACE A WITHIN .001"
3. DIA D & E TO BE CONCENTRIC WITHIN .006

THERMOELECTRIC SPECIFICATIONS FOR Ge-Si-THERMOCOUPLES

(1) Cold junction operating temperature: 500°C (see notes (a) + (b)).

(2) Hot junction operating temperature: 1000°C (see note (c)).

(3) Potential output between 850°C and 500°C: 200 mv ± 15%.

(4) Over-all couple efficiency for operation between 850°C and 500°C: 3.5 - 4.5% (see note (d)).

(5) Couple lifetime: 5 years (see note (e)).

(6) Allowable output degradation of couples during life: 15% max, (see notes (e) + (f)).

NOTES ON SPECIFICATIONS

(a) The cold junction terminal shall be tungsten.

(b) Although the cold junction operating temperature is set at 500°C, the whole couple assembly must withstand short term heating (~ 30 min.) to 850°C.

(c) The hot junction must be potentially capable of being operated at 1000°C. Any limitations regarding contacting of the hot strap at that temperature should be specified by the seller.

(d) Over-all couple efficiency denotes the total thermal to electrical conversion efficiency for the couple as presently dimensioned (see attached drawing) for operation between 850°C and 500°C including Carnot losses.

(e) Life time and output degradation predictions shall be based on life tests of not less than 2 years duration.

(f) The output degradation factor shall be equally applicable to potential and efficiency.

ACTUAL SIZE

QTY PER DASH NO.	PART OR IDENTIFYING NO.	NOMENCLATURE OR DESCRIPTION	NOTE	ITEM NO.

PARTS LIST

UNLESS OTHERWISE SPECIFIED DIMENSIONS ARE IN INCHES TOLERANCES ANGLES ± DECIMALS 2 PLACE ± 3 PLACE ±.004 SURFACES √ MICRO-INCHES	DR A Bell 7 Feb 69 CHK S Marmelstein 2/12/69 APPD H E Bates 12 Feb 69 APPD [illegible] 12 Feb. 69	TYCO LABORATORIES, INC.	
FINISH NEXT ASSEMBLY | MODEL	MATERIAL HOT SHOE MATL: -1: HIGH DOPED SILICON -2. MOLYBDENUM DISILICIDE	APPLICABLE DOCUMENTS	Si-Ge - THERMOCOUPLE SIZE 567-200 SCALE 4/1 SHEET 1 OF 1

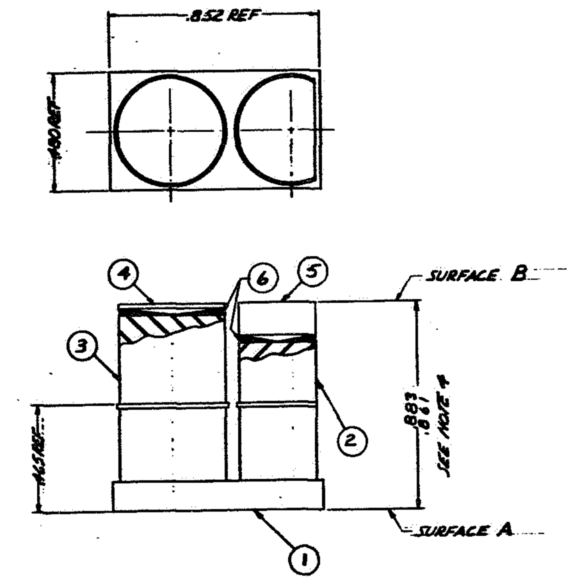

NOTES:
1. BOND ITEM 1 TO ITEMS 3 & 4 USING PROCESS NO. 567-2000 AND FIXTURE NO. 567-2000-1
2. "TIN" ITEMS 4 & 5 USING PROCESS NO. 567-2001 & FIXTURE NO. 567-2000-2
3. SWEAT COUPLE SUB-ASSY (ITEMS 1, 2 & 3) TO ITEMS 4 & 5 USING PROCESS NO. 567-2003 AND FIXTURE NO. 567-2000-3
4. SURFACE A & B TO BE PARALLEL WITHIN .001

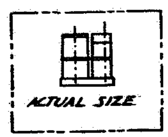

REVISIONS

SYM	ZONE	DESCRIPTION	DATE	APPROVED

PARTS LIST

QTY PER DASH NO. -1	PART OR IDENTIFYING NO.	NOMENCLATURE OR DESCRIPTION	ITEM NO.
AR		SOLDER (HIGH TEMP)	6
1	567-205	SHOE TYPE P	5
1	567-204	SHOE, TYPE N	4
1	567-203	ELEMENT, LEAD TELLURIDE 3N	3
1	567-202	ELEMENT, LEAD TELLURIDE 3P	2
1	567-200	Si-Ge - THERMOCOUPLE	1

UNLESS OTHERWISE SPECIFIED DIMENSIONS ARE IN INCHES
TOLERANCES
ANGLES ±
DECIMALS
2 PLACE ±
3 PLACE ±
SURFACES √ MICRO-INCHES
MATERIAL
FINISH
NEXT ASSEMBLY 567-206
MODEL

DR. [illegible] 21 Feb 62
CHK [illegible] 2/21/[illegible]
APPD [illegible] 2/27/[illegible]
APPD
APPLICABLE DOCUMENTS

TYCO LABORATORIES, INC.

Si-Ge-PbTe SEGMENTED COUPLE

SIZE D 567-201

SCALE 4/1 SHEET 1 OF 1

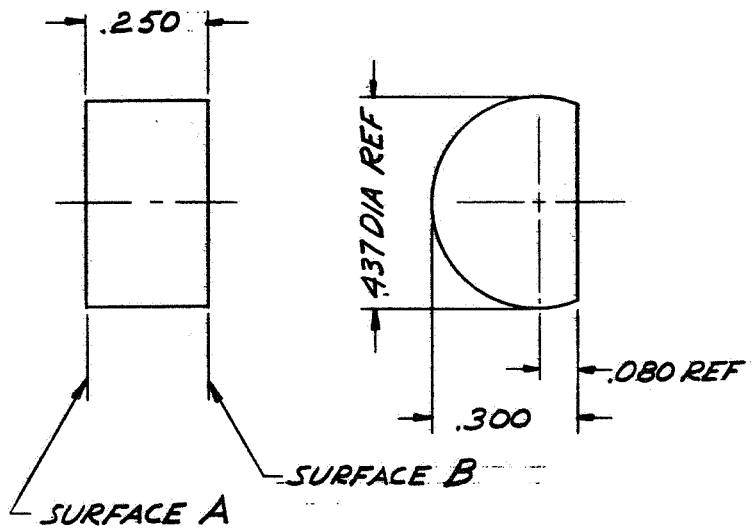

NOTES:
1. SURFACE A & B TO BE PARALLEL WITHIN .002
2. SURFACE A & B TO BE FLAT WITHIN .001

REVISIONS				
SYM	ZONE	DESCRIPTION	DATE	APPROVED

REV

QTY PER DASH NO.	PART OR IDENTIFYING NO.	NOMENCLATURE OR DESCRIPTION	NOTE	ITEM NO.

PARTS LIST

UNLESS OTHERWISE SPECIFIED DIMENSIONS ARE IN INCHES

TOLERANCES
ANGLES ±
DECIMALS
2 PLACE ±
3 PLACE ± .005

SURFACES √ MICRO-INCHES

DR L. Bellow DATE 18 Feb 69
CHK S. Merrill 2/27/69
APPD S. Merrill 2/27/69
APPD

TYCO LABORATORIES, INC.

ELEMENT, LEAD TELLURIDE 3P

FINISH

MATERIAL
TEGS-3P
LEAD TELLURIDE
3M COMPANY

APPLICABLE DOCUMENTS

NEXT ASSEMBLY 567-201 | MODEL

SIZE B | 567-202

SCALE 4/1 | SHEET 1 OF 1

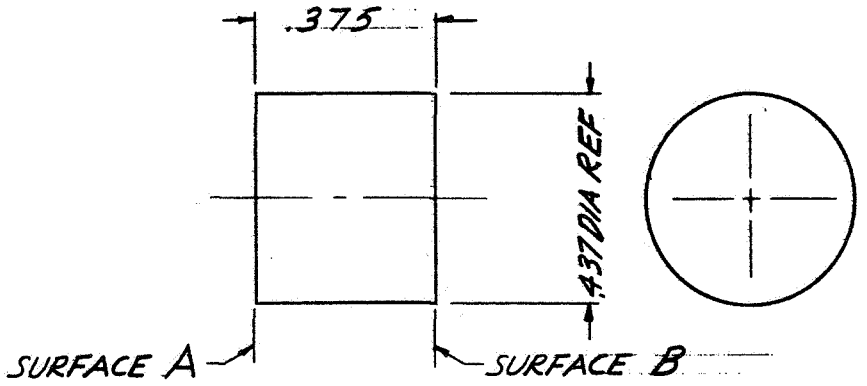

NOTES:
1. SURFACE A & B TO BE PARALLEL WITHIN .002
2. SURFACE A & B TO BE FLAT WITHIN .001

REVISIONS				
SYM	ZONE	DESCRIPTION	DATE	APPROVED

REV

QTY PER DASH NO.	PART OR IDENTIFYING NO.	NOMENCLATURE OR DESCRIPTION	NOTE	ITEM NO.

PARTS LIST

UNLESS OTHERWISE SPECIFIED DIMENSIONS ARE IN INCHES

TOLERANCES
ANGLES ±
DECIMALS
2 PLACE ±
3 PLACE ±.005

SURFACES √ MICRO-INCHES

DR L. Bellow 18 Feb 69
CHK S. Marcus 2/27/69
APPD S. Marcus 2/27/69
APPD

TYCO LABORATORIES, INC.

ELEMENT, LEAD TELLURIDE
3N

FINISH

MATERIAL
TEGS-3N
LEAD TELLURIDE
3M COMPANY

APPLICABLE DOCUMENTS

NEXT ASSEMBLY 567-201
MODEL

SIZE B
567-203

SCALE 4/1
SHEET 1 OF 1

REVISIONS				
SYM	ZONE	DESCRIPTION	DATE	APPROVED

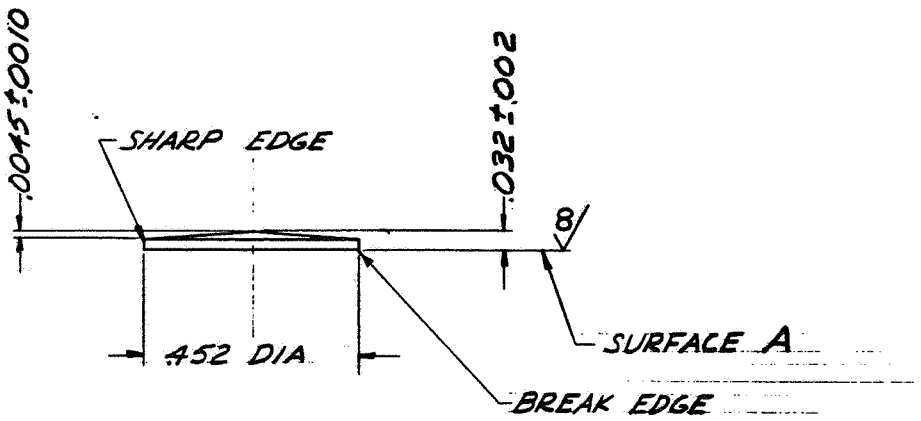

NOTES:
1. SURFACE A TO BE FLAT WITHIN .00005

REV

QTY PER DASH NO.	PART OR IDENTIFYING NO.	NOMENCLATURE OR DESCRIPTION	NOTE	ITEM NO.

PARTS LIST

UNLESS OTHERWISE SPECIFIED DIMENSIONS ARE IN INCHES TOLERANCES ANGLES ± DECIMALS 2 PLACE ± 3 PLACE ±.005 SURFACES √ MICRO-INCHES	DR L Bellow DATE 19 Feb 69 CHK S. Merrell 2/27/69 APPD S. Merrotto 2/27/69 APPD	TYCO LABORATORIES, INC. SHOE, TYPE N	
FINISH GOLD PLATE .0003 THK ±.000025	MATERIAL COPPER	APPLICABLE DOCUMENTS	SIZE B 567-204
NEXT ASSEMBLY 567-201 / MODEL			SCALE 4/1 / SHEET 1 OF 1

REVISIONS				
SYM	ZONE	DESCRIPTION	DATE	APPROVED

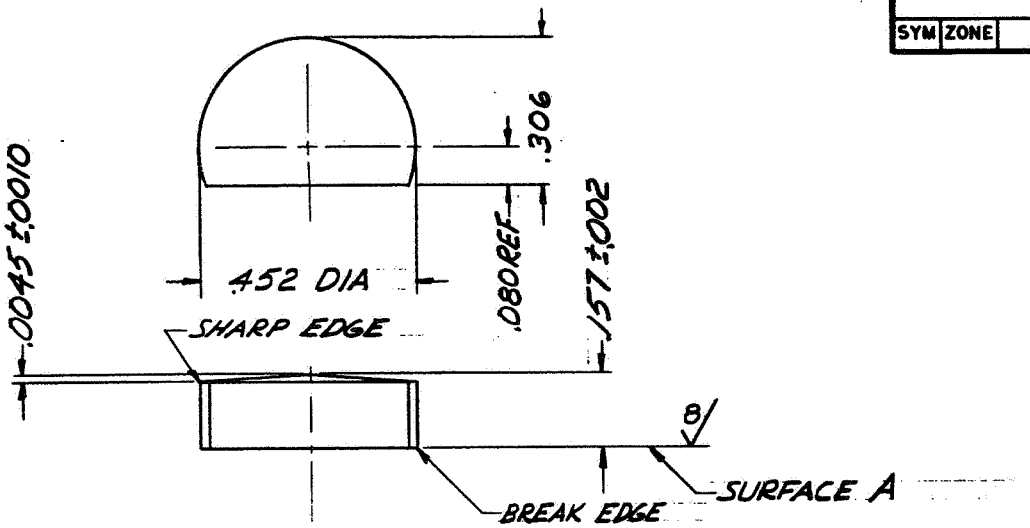

REV

NOTES:
1. SURFACE A TO BE FLAT WITHIN .00005

QTY PER DASH NO.	PART OR IDENTIFYING NO.	NOMENCLATURE OR DESCRIPTION	NOTE	ITEM NO.

PARTS LIST

UNLESS OTHERWISE SPECIFIED DIMENSIONS ARE IN INCHES
TOLERANCES
ANGLES ±
DECIMALS
2 PLACE ±
3 PLACE ±.005
SURFACES 63/ MICRO-INCHES

DR L Bellow DATE 19 Feb 69
CHK S. Merrill 2/27/69
APPD S. Merrill 2/27/69
APPD

TYCO LABORATORIES, INC.

SHOE, TYPE P

FINISH: GOLD PLATE .0003 THK ±.000025
MATERIAL: COPPER
APPLICABLE DOCUMENTS

NEXT ASSEMBLY: 567-201
MODEL:

SIZE B | 567-205
SCALE 4/1 | SHEET 1 OF 1

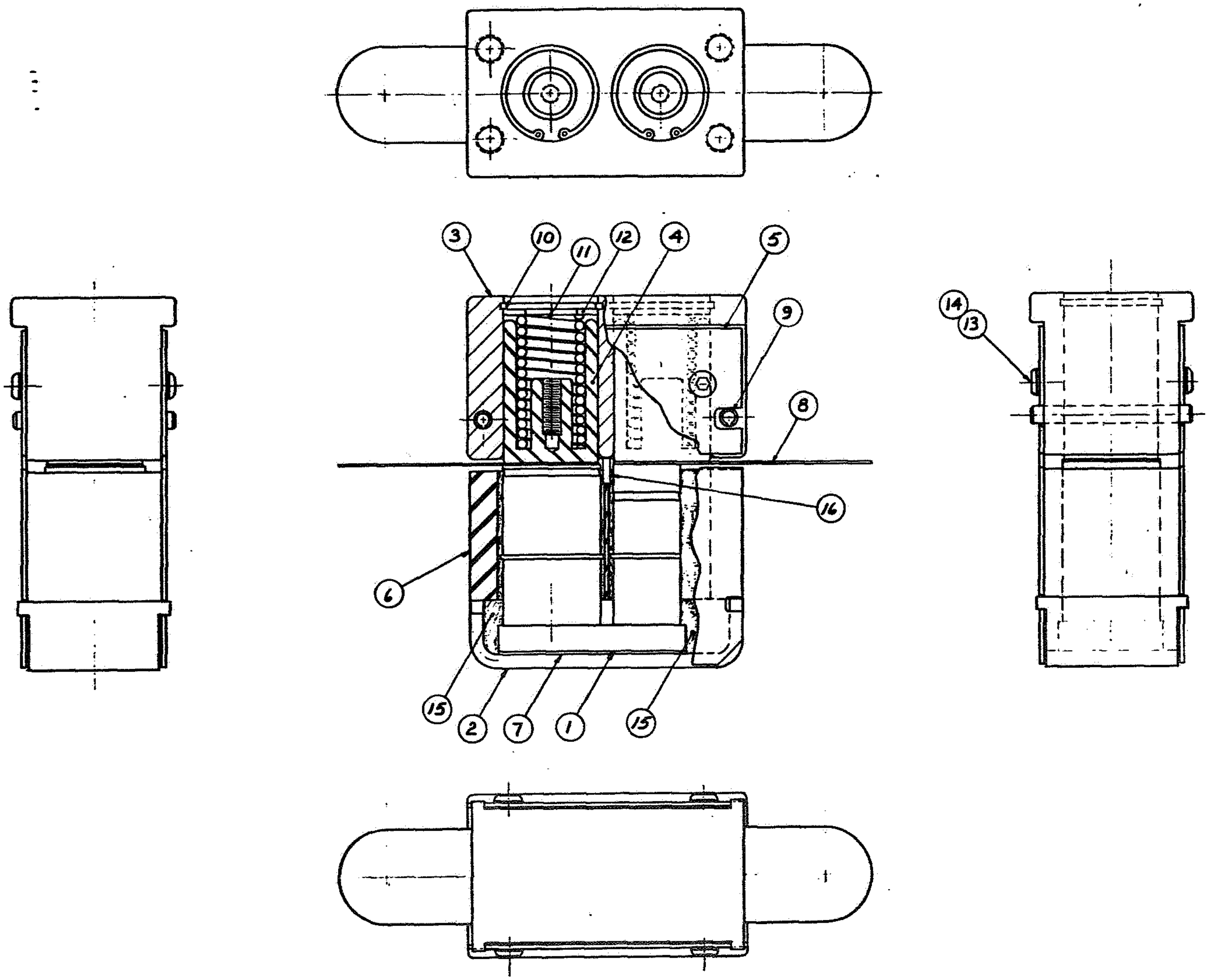

QTY PER DASH NO.	PART OR IDENTIFYING NO.	NOMENCLATURE OR DESCRIPTION	NOTE	ITEM NO.
1	567-214	SPACER,		16
AR	6#/FT³ DENSITY	MICRO-QUARTZ FELT (JOHNS-MANVILLE)		15
6		WASHER NO."D" .010 THK. LEAD		14
6		SCREW, BUTTON HD. CRES NO. 0-80 X 1/2 LG		13
2		WASHER, FLAT NO. 6 LIGHT CRES .030 THK		12
2	LC-038D-15	SPRING, COMPRESSION-CRES (LEE)		11
2	N5000-43-H	RING, RETAINING INTERNAL (WALDES)		10
2		ROLL PIN .078 DIA X .75 LG (ESNA) CRES		9
2	567-212	STRAP, INTERCONNECTION		8
1	567-213	INSULATOR		7
1	567-211	INSULATOR BLOCK		6
2	567-210	PLATE, SIDE		5
2	567-209	PISTON		4
1	567-208	COLD SHOE		3
1	567-207	HOT SHOE		2
1	567-201	Si-Ge-PbTe SEGMENTED COUPLE		1

PARTS LIST

UNLESS OTHERWISE SPECIFIED DIMENSIONS ARE IN INCHES
TOLERANCES: ANGLES ± — DECIMALS 2 PLACE ± — 3 PLACE ± —
SURFACES √ MICRO-INCHES
DR L. Bitler DATE 21 Feb 67
CHK S. Permin 2/27/67
APPD S. Permin 2/ /67
MATERIAL —
FINISH —
APPLICABLE DOCUMENTS

TYCO LABORATORIES, INC.

THERMOELECTRIC BUILDING BLOCK MODULE ASSEMBLY

SIZE D 567-206

SCALE 4/1 SHEET 1 OF 1

REVISIONS				
SYM	ZONE	DESCRIPTION	DATE	APPROVED

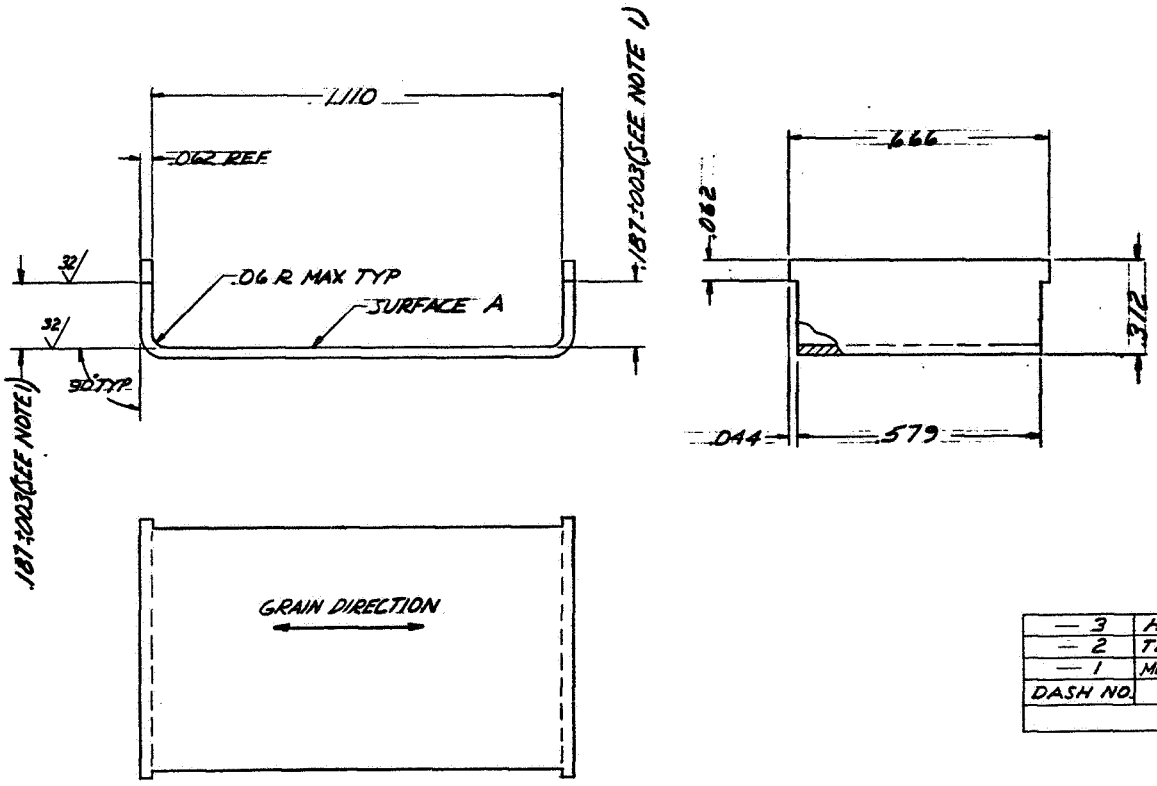

DASH NO.	MATERIAL
— 3	H.T. MOLYBDENUM .040 THK (NORTON CO.)
— 2	TZM MOLYBDENUM .062 ±.002 THK
— 1	MOLYBDENUM STRIP ANNEALED .062 ±.002 THK

VARIATIONS

NOTES:
1. NOMINAL .187 DIM MUST NOT VARY MORE THAN .0001 FROM END TO END
2. SURFACE A TO BE FLAT WITHIN .0001
3. BREAK ALL EDGES

QTY PER DASH NO.	PART OR IDENTIFYING NO.	NOMENCLATURE OR DESCRIPTION	NOTE	ITEM NO.

PARTS LIST

UNLESS OTHERWISE SPECIFIED DIMENSIONS ARE IN INCHES
TOLERANCES
ANGLES ± ½°
DECIMALS
2 PLACE ±.02
3 PLACE ±.005
SURFACES 125 √ MICRO-INCHES

DR J. Bellow 20 Feb 69
CHK S. Hamilton 2/27/69
APPD S. Hamilton 2/27/69
APPD

TYCO LABORATORIES, INC.

HOT SHOE

FINISH

MATERIAL
SEE DASH VARIATIONS

APPLICABLE DOCUMENTS

NEXT ASSEMBLY 567-206
MODEL

SIZE C
567-207
SCALE 4/1
SHEET 1 OF 1

K+E

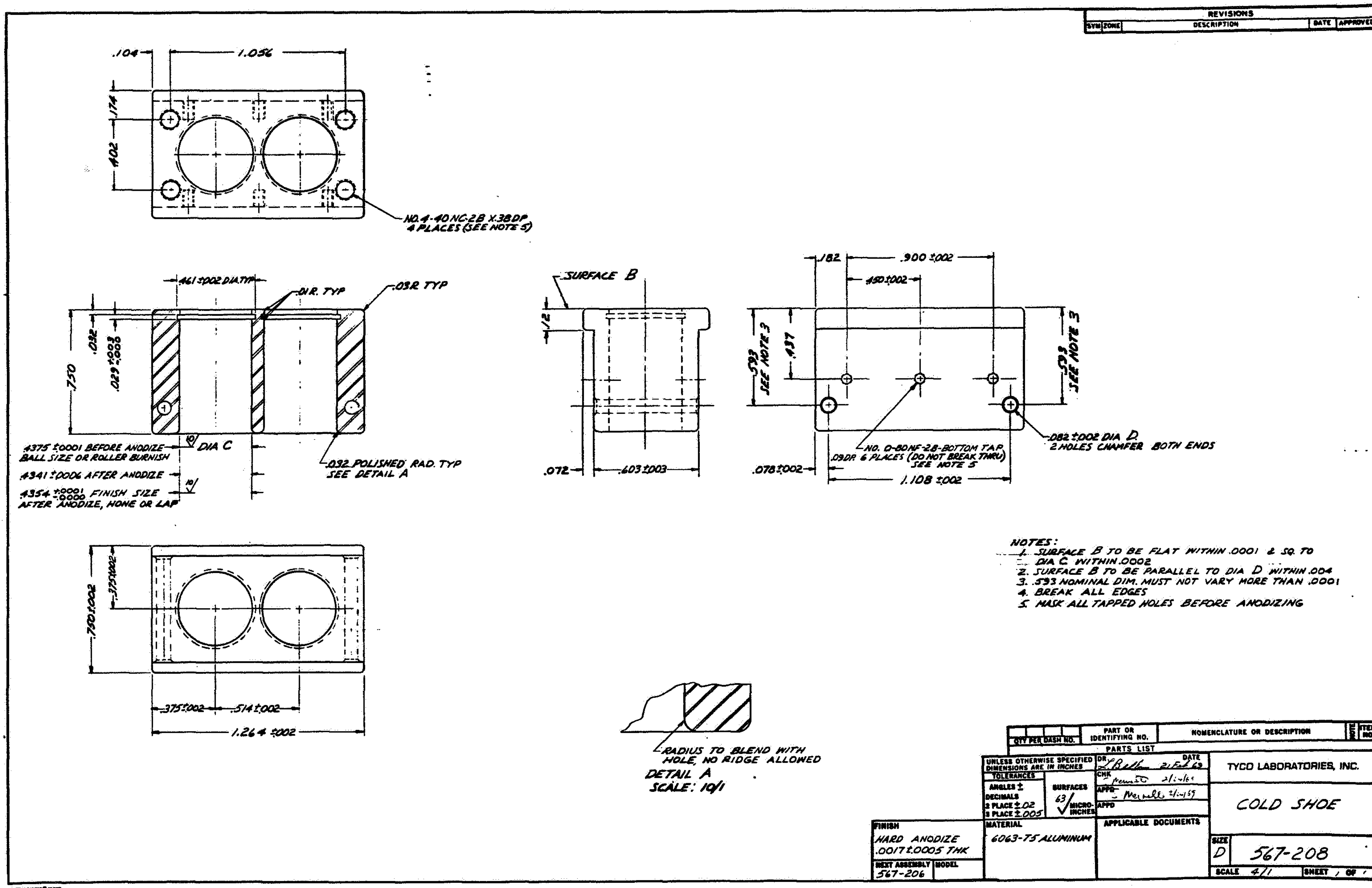

REVISIONS
SYM ZONE DESCRIPTION DATE APPROVED
.104
1.056
.174
.402
NO. 4-40 NC-2B X .38 DP
4 PLACES (SEE NOTE 5)
.461 ±.002 DIA TYP
.01 R. TYP
.03 R TYP
.750
.032
.029 +.003 -.000
DIA C
.4375 ±.0001 BEFORE ANODIZE
BALL SIZE OR ROLLER BURNISH
.4341 ±.0006 AFTER ANODIZE
.4354 +.0001 -.0000 FINISH SIZE
AFTER ANODIZE, HONE OR LAP
.032 POLISHED RAD. TYP
SEE DETAIL A
SURFACE B
.12
.072
.603 ±.003
.182
.900 ±.002
.450 ±.002
.593 SEE NOTE 3
.437
NO. 0-80NF-2B-BOTTOM TAP
.09 DP. 6 PLACES (DO NOT BREAK THRU)
SEE NOTE 5
.082 ±.002 DIA D
2 HOLES CHAMFER BOTH ENDS
.078 ±.002
1.108 ±.002
.375 ±.002
.750 ±.002
.375 ±.002
.514 ±.002
1.264 ±.002
NOTES:
1. SURFACE B TO BE FLAT WITHIN .0001 & SQ. TO DIA C WITHIN .0002
2. SURFACE B TO BE PARALLEL TO DIA D WITHIN .004
3. .593 NOMINAL DIM. MUST NOT VARY MORE THAN .0001
4. BREAK ALL EDGES
5. MASK ALL TAPPED HOLES BEFORE ANODIZING
RADIUS TO BLEND WITH HOLE, NO RIDGE ALLOWED
DETAIL A
SCALE: 10/1
QTY PER DASH NO.
PART OR IDENTIFYING NO.
NOMENCLATURE OR DESCRIPTION
NOTE
ITEM NO.
PARTS LIST
UNLESS OTHERWISE SPECIFIED DIMENSIONS ARE IN INCHES
TOLERANCES
ANGLES ±
DECIMALS
2 PLACE ±.02
3 PLACE ±.005
SURFACES
63 MICRO-INCHES
DR
DATE
21 Feb 69
CHK
APPD
APPD
APPLICABLE DOCUMENTS
TYCO LABORATORIES, INC.
COLD SHOE
FINISH
HARD ANODIZE
.0017 ±.0005 THK
MATERIAL
6063-T5 ALUMINUM
NEXT ASSEMBLY
567-206
MODEL
SIZE
D
567-208
SCALE 4/1
SHEET 1 OF 1

REVISIONS				
SYM	ZONE	DESCRIPTION	DATE	APPROVED

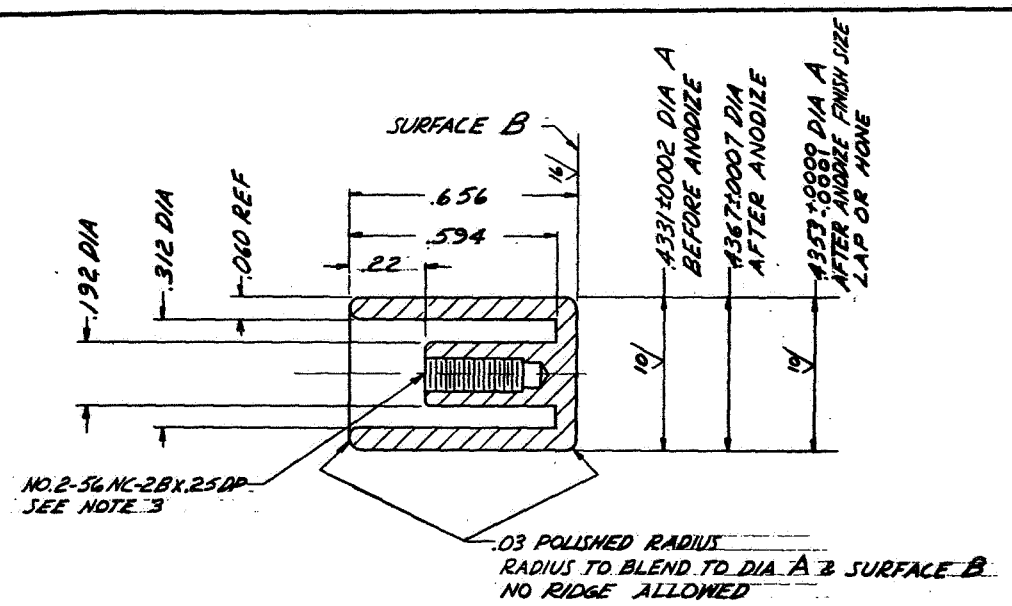

NOTES:
1. SURFACE B TO BE FLAT WITHIN .0001 & SQ. TO DIA A WITHIN .0001
2. BREAK ALL EDGES
3. MASK TAPPED HOLE BEFORE ANODIZING

QTY PER DASH NO.				PART OR IDENTIFYING NO.	NOMENCLATURE OR DESCRIPTION	NOTE	ITEM NO.

PARTS LIST

UNLESS OTHERWISE SPECIFIED DIMENSIONS ARE IN INCHES
TOLERANCES
ANGLES ±
DECIMALS
2 PLACE ±.02
3 PLACE ±.005
SURFACES 63 √ MICRO-INCHES

DR L Bell 21 Feb 69
CHK J. Merritt 2/27/69
APPD J. Merritt 2/27/69
APPD

TYCO LABORATORIES, INC.

PISTON

FINISH	MATERIAL	APPLICABLE DOCUMENTS
HARD ANODIZE .0018±.0005 THK	6063-T5 ALUMINUM	

NEXT ASSEMBLY: 567-206 | MODEL:

SIZE C | 567-209

SCALE 4/1 | SHEET 1 OF 1

REVISIONS				
SYM	ZONE	DESCRIPTION	DATE	APPROVED

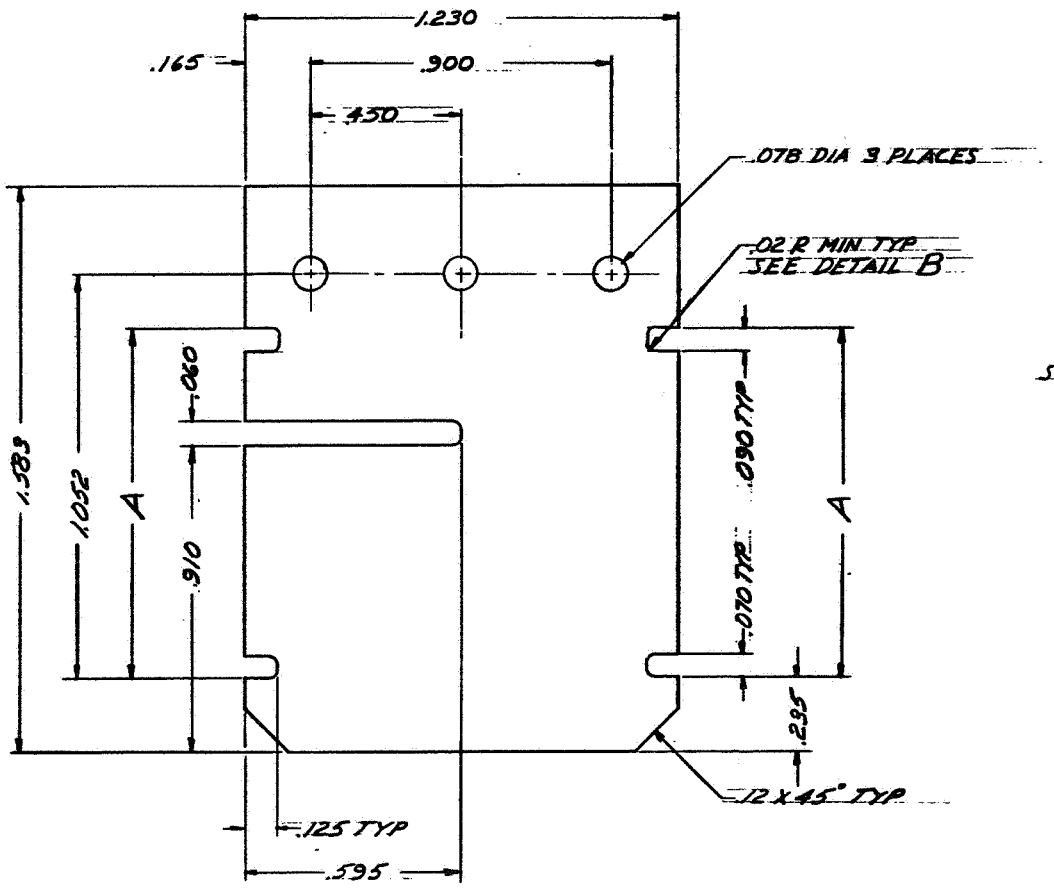

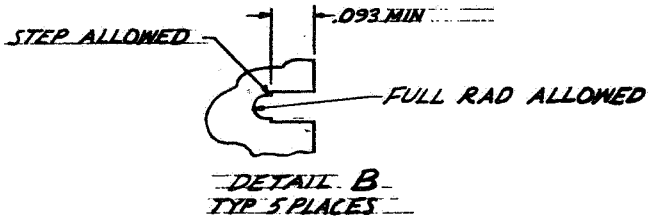

— 2	.935±.005	SEE NOTE 2
— 1	.935±.005	
DASH NO.	A DIM	
VARIATIONS		

NOTES:
1. MAX. CAMBER NOT TO EXCEED .004
2. DIM A ±.005 MUST NOT VARY MORE THAN .0002 FROM SIDE TO SIDE (NOTE: -2 VARIATION ONLY)

QTY PER DASH NO.	PART OR IDENTIFYING NO.	NOMENCLATURE OR DESCRIPTION	NOTE	ITEM NO.

PARTS LIST

UNLESS OTHERWISE SPECIFIED DIMENSIONS ARE IN INCHES
TOLERANCES
ANGLES ± 1°
DECIMALS
2 PLACE ±
3 PLACE ±.005
SURFACES
√ MICRO-INCHES

DR L Bellow 2/6/64 DATE
CHK S. Manolatos 2/27/64
APPD S. Manolatos 2/27/64
APPD

TYCO LABORATORIES, INC.

PLATE, SIDE

FINISH

MATERIAL
.020 ±.002 THK
STEATITE

APPLICABLE DOCUMENTS

NEXT ASSEMBLY 567-206
MODEL

SIZE C
567-210
SCALE 4/1
SHEET 1 OF 1

REVISIONS				
SYM	ZONE	DESCRIPTION	DATE	APPROVED

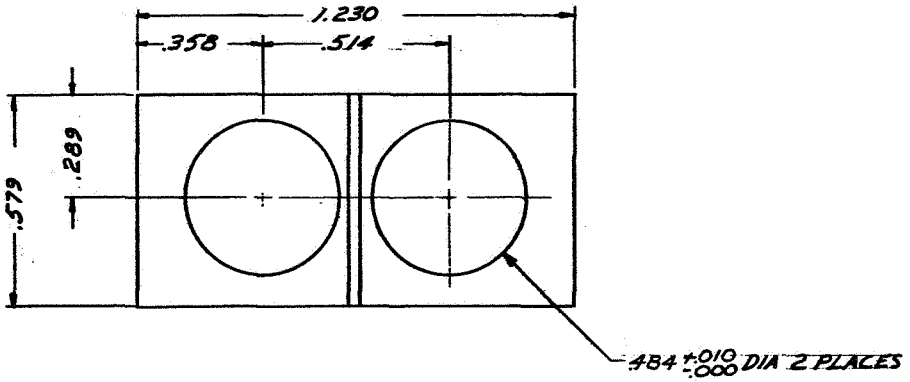

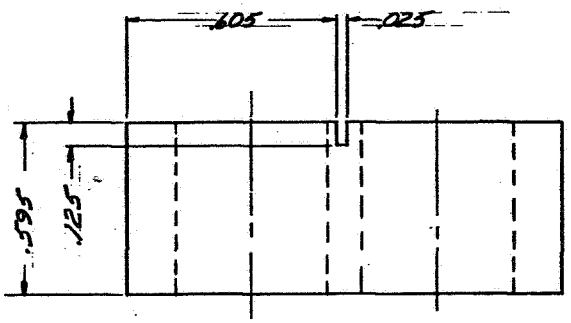

NOTES.
1. BREAK OUT OF MATL. NOT EXCEEDING 1/16 x 1/8 IS ACCEPTABLE

QTY PER DASH NO.	PART OR IDENTIFYING NO.	NOMENCLATURE OR DESCRIPTION	NOTE	ITEM NO.

PARTS LIST

UNLESS OTHERWISE SPECIFIED DIMENSIONS ARE IN INCHES TOLERANCES ANGLES ± DECIMALS 2 PLACE ± 3 PLACE ± .005	SURFACES √ MICRO-INCHES	DR L. Bellow 2/25/69 CHK S. Marcus 2/27/69 APPD S. Marcus 2/27/69 APPD	TYCO LABORATORIES, INC. INSULATOR BLOCK
FINISH NEXT ASSEMBLY 567-206 MODEL	MATERIAL MIN-K 2000 (JOHNS-MANVILLE CO.)	APPLICABLE DOCUMENTS	SIZE C 567-211 SCALE 4/1 SHEET 1 OF 1

REVISIONS				
SYM	ZONE	DESCRIPTION	DATE	APPROVED

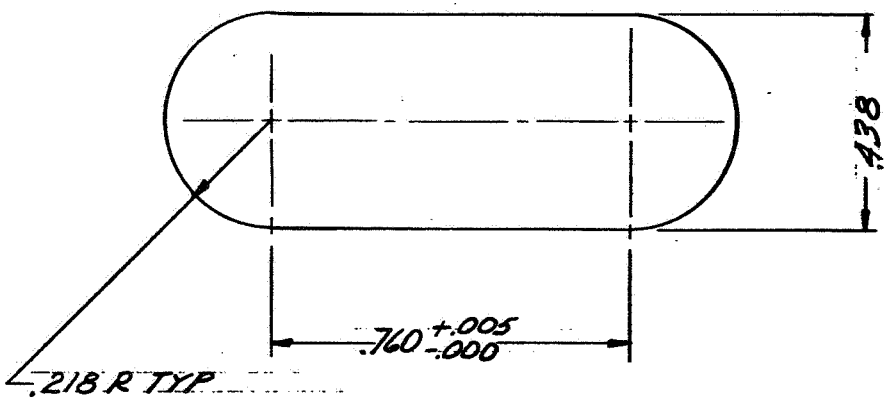

REV

QTY PER DASH NO.	PART OR IDENTIFYING NO.	NOMENCLATURE OR DESCRIPTION	NOTE	ITEM NO.

PARTS LIST

UNLESS OTHERWISE SPECIFIED DIMENSIONS ARE IN INCHES

TOLERANCES

ANGLES ±

DECIMALS

2 PLACE ±

3 PLACE ± .005

SURFACES √ MICRO-INCHES

DR L. Bellows 21 Feb 69 DATE

CHK S. Merrett 2/24/69

APPD S. Merrett 2/24/69

APPD

TYCO LABORATORIES, INC.

STRAP, INTERCONNECTION

SIZE B

567-212

SCALE 4/1

SHEET 1 OF 1

FINISH

NONE

MATERIAL

FINE SILVER, ANNEALED

.010 ±.0002 THK

APPLICABLE DOCUMENTS

NEXT ASSEMBLY 567-206

MODEL

REVISIONS				
SYM	ZONE	DESCRIPTION	DATE	APPROVED

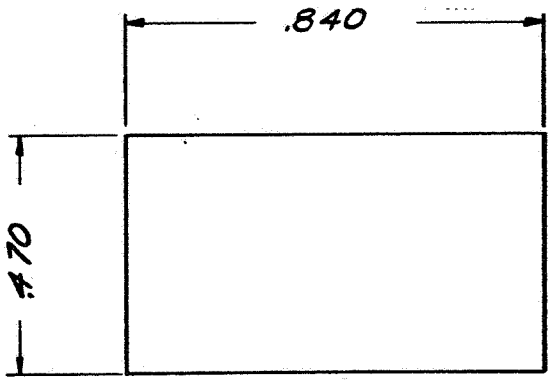

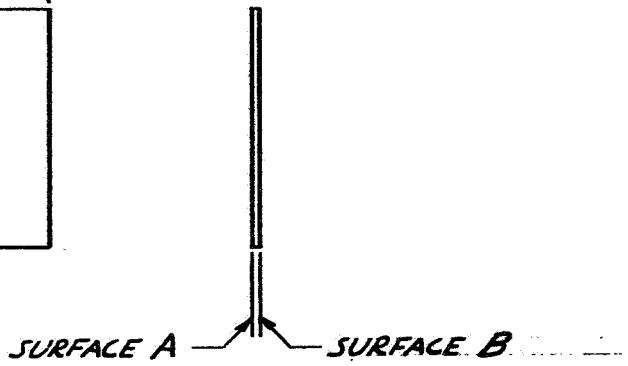

REV

NOTES:
1. SURFACE A & B TO BE FLAT AND PARALLEL WITHIN .0001

QTY PER DASH NO.				PART OR IDENTIFYING NO.	NOMENCLATURE OR DESCRIPTION	NOTE	ITEM NO.

PARTS LIST

UNLESS OTHERWISE SPECIFIED DIMENSIONS ARE IN INCHES

TOLERANCES
ANGLES ±
DECIMALS
2 PLACE ± —
3-PLACE ± .005

SURFACES √ MICRO-INCHES

DR L. Bellow DATE 27 Feb 69
CHK S. Merrill 2/27/69
APPD S. Merrill 2/27/69
APPD

TYCO LABORATORIES, INC.

INSULATOR

FINISH —

MATERIAL
.010 ± .002 THK
99.5% ALUMINA

APPLICABLE DOCUMENTS

NEXT ASSEMBLY 567-206

MODEL

SIZE B

567-213

SCALE 4/1

SHEET 1 OF 1

REVISIONS				
SYM	ZONE	DESCRIPTION	DATE	APPROVED

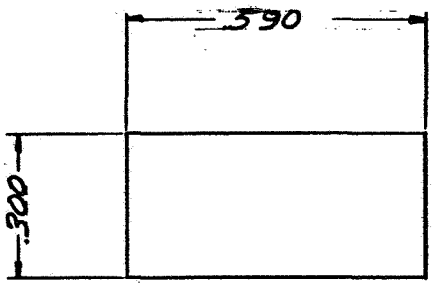

QTY PER DASH NO.	PART OR IDENTIFYING NO.	NOMENCLATURE OR DESCRIPTION	NOTE	ITEM NO.

PARTS LIST

UNLESS OTHERWISE SPECIFIED DIMENSIONS ARE IN INCHES

TOLERANCES

ANGLES ±

DECIMALS

2 PLACE ±

3 PLACE ±.005

SURFACES

√ MICRO-INCHES

DR L. Bellar DATE 27 Feb 69

CHK S. Mennga 2/27/69

APPD S. Mennga 2/27/69

APPD

TYCO LABORATORIES, INC.

SPACER

FINISH

MATERIAL

.020 ±.002 STEATITE

APPLICABLE DOCUMENTS

NEXT ASSEMBLY 567-206

MODEL

SIZE B

567-214

SCALE 4/1

SHEET 1 OF 1

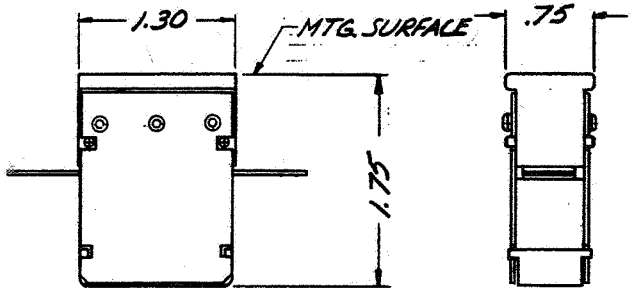

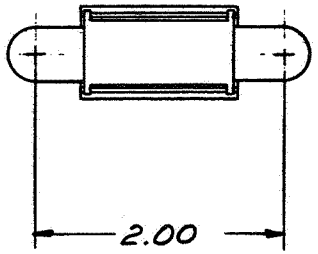

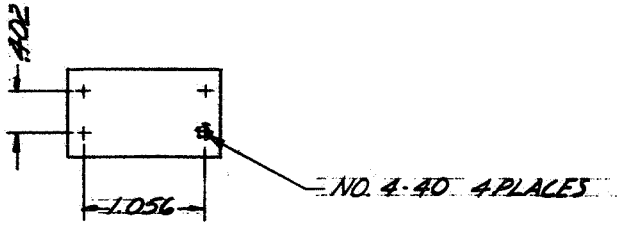

MTG. DIM'S

REVISIONS				
SYM	ZONE	DESCRIPTION	DATE	APPROVED

REV

QTY PER DASH NO.				PART OR IDENTIFYING NO.	NOMENCLATURE OR DESCRIPTION	NOTE	ITEM NO.

PARTS LIST

UNLESS OTHERWISE SPECIFIED DIMENSIONS ARE IN INCHES

TOLERANCES

ANGLES ± —

DECIMALS

2 PLACE ± —

3 PLACE ± —

SURFACES √ MICRO-INCHES

DR L Bellomo DATE 27 Feb 69

CHK

APPD

APPD

TYCO LABORATORIES, INC.

THERMOELECTRIC BUILDING BLOCK MODULE OUTLINE

FINISH —

MATERIAL —

APPLICABLE DOCUMENTS

NEXT ASSEMBLY | MODEL

SIZE B | 567-215

SCALE 1/1 | SHEET 1 OF 1